

**Stable Enols of Amides ArNHC(OH)=C(CN)CO<sub>2</sub>R. *E/Z* Enols, Equilibria with the Amides, Solvent Effects, and Hydrogen Bonding**

Yi Xiong Lei,<sup>†</sup> Daniele Casarini,<sup>‡</sup> Giovanni Cerioni,<sup>§</sup> and Zvi Rappoport<sup>\*,†</sup>

Department of Organic Chemistry, The Hebrew University, Jerusalem 91904, Israel; Chemistry Department, University of Basilicata, 80100 Potenza, Italy; Dipartimento Farmaco Chimico Tecnologico, Università di Cagliari, I-09124 Cagliari, Italy

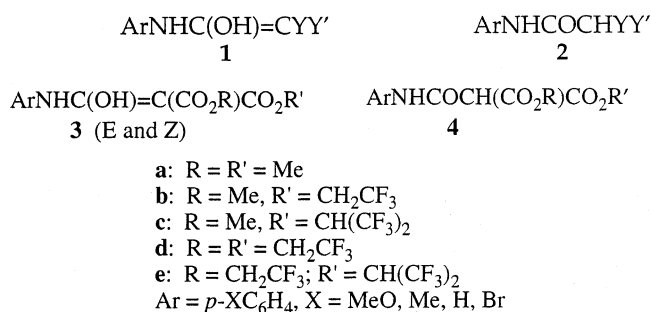
zr@vms.huji.ac.il

Received July 11, 2002

The structures of anilido cyano(fluoroalkoxycarbonyl)methanes ArNHCOCH(CN)CO<sub>2</sub>R, where R = CH<sub>2</sub>CF<sub>3</sub> or CH(CF<sub>3</sub>)<sub>2</sub>, Ar = *p*-XC<sub>6</sub>H<sub>4</sub>, and X = MeO, Me, H, or Br, were investigated. In the solid state, all exist as the enols ArNHC(OH)=C(CN)CO<sub>2</sub>R **7** (R = CH<sub>2</sub>CF<sub>3</sub>) and **9** (R = CH(CF<sub>3</sub>)<sub>2</sub>) with cis arrangement of the hydrogen-bonded ROC=O...HO moiety and a long C1=C2 bond. The product composition in solution is solvent dependent. In CDCl<sub>3</sub> solution, only a single enol is observed, whereas in THF-*d*<sub>6</sub> and CD<sub>3</sub>CN, two enols (*E* and *Z*) are the major products, and the amide is the minor product or not observed at all (*K*<sub>Enol</sub> 1.04–9 (CD<sub>3</sub>CN, 298 K) and 3 to ≥100 (THF, 300 K)). The percentage of the amide and the *Z*-enol increase upon an increase in temperature. In all solvents, the percent enol is higher for **9** than for **7**. In CD<sub>3</sub>CN, more enol is observed when the aryl group is more electron-donating. The spectra in DMSO-*d*<sub>6</sub> and DMF-*d*<sub>7</sub> indicate the presence of mostly a single species, whose spectra do not change on addition of a base and is ascribed to the anion of the ionized carbon acid. Comparison with systems where the CN is replaced by a CO<sub>2</sub>R group (R = CH<sub>2</sub>CF<sub>3</sub>, CH(CF<sub>3</sub>)<sub>2</sub>) shows a higher percentage of enol for the CN-substituted system. Intramolecular (to CO<sub>2</sub>R) and intermolecular hydrogen bonds determine, to a significant extent, the stability of the enols, their *Z/E* ratios (e.g., *Z/E* (THF, 240 K) = 3.2–4.0 (**7**) and 0.9–1.3 (**9**)), and their δ(OH) in the <sup>1</sup>H spectra. The interconversion of *Z*- and *E*-enol by rotation around the C=C bond was studied by DNMR, and Δ*G*<sup>‡</sup> values of ≥15.3 and 14.1 ± 0.4 kcal/mol for **Z-7** and **Z-9** were determined. Features of the NMR spectra of the enols and their anions are discussed.

**Introduction**

Our previous investigations on stable enols of carboxamides activated by two electron-withdrawing groups (EWG)Y,Y' (**1**)<sup>1–3</sup> had shown that with Y,Y' = CO<sub>2</sub>R, CO<sub>2</sub>R', equilibria with the amides **2** is established in solution and that several of the **1/2** systems exist as enols **1** in the solid state. A systematic change by replacing the Y = Y' = CO<sub>2</sub>Me groups by the ester groups CO<sub>2</sub>CH<sub>2</sub>CF<sub>3</sub> and CO<sub>2</sub>CH(CF<sub>3</sub>)<sub>2</sub> with an increasing number of fluorines had shown that the percentage of the enol **3**, i.e., in the **3/4** mixture expressed as *K*<sub>Enol</sub> = [**1**]/[**2**] at equilibrium increases when Y,Y' become more electron withdrawing (**3e** > **3d** > **3c** > **3b** > **3a**). Systems with ≥6 fluorines in Y,Y'<sup>3</sup> or when YY' is a Meldrum's acid residue<sup>1</sup> exist in the solid as the enols **3**. When the polarity of the solvent is increased from CCl<sub>4</sub> and CDCl<sub>3</sub> to CD<sub>3</sub>CN and DMSO-



*d*<sub>6</sub>, *K*<sub>Enol</sub> decreases. Whereas in the chlorinated solvents the enols are mostly the major component, they are observed only for the highly fluorinated systems in CD<sub>3</sub>CN, and no enol was observed in DMSO-*d*<sub>6</sub>. *E*- and *Z*-enols were observed in solution for **3b,c,e**. DFT calculations<sup>4</sup> had shown that the enols are stabilized by β-EWGs, presumably by the contribution of the push-pull valence bond hybrid **1a** of the enol, with a consequent increase in *K*<sub>Enol</sub>. These groups also destabilize the amide form **2** (presumably by dipole–dipole CO/Y,Y'

\* To whom correspondence should be addressed.

<sup>†</sup> The Hebrew University

<sup>‡</sup> University of Basilicata

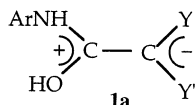
<sup>§</sup> Università di Cagliari

(1) Mukhopadhyaya, J. K.; Sklenak, S.; Rappoport, Z. *J. Am. Chem. Soc.* **2000**, *122*, 1325.

(2) Mukhopadhyaya, J. K.; Sklenak, S.; Rappoport, Z. *J. Org. Chem.* **2000**, *65*, 6856.

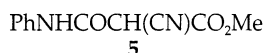
(3) Lei, Y. X.; Cerioni, G.; Rappoport, Z. *J. Org. Chem.* **2001**, *66*, 8379.

(4) (a) Sklenak, S.; Apeloig, Y.; Rappoport, Z. *J. Am. Chem. Soc.* **1998**, *120*, 10359. (b) Rappoport, Z.; Lei, Y. X.; Yamataka, H. *Helv. Chim. Acta* **2001**, *84*, 1405.



interaction<sup>4b</sup>), thus contributing to the increase in  $K_{\text{Enol}}$ . Hydrogen bonding between the enolic OH group and the group Y and/or Y' was also deduced to be of major importance in stabilizing the enols<sup>1,3</sup> and in affecting  $K_{\text{Enol}}$ , the relative *E/Z* ratios when  $Y \neq Y'$ , and the  $\delta$ -(OH) and  $\delta$ -(NH) chemical shifts.<sup>3</sup>

Extensions to other systems where both  $Y, Y' \neq \text{CO}_2\text{R}$ ,  $\text{CO}_2\text{R}'$  are so far limited. Two cyano groups ( $Y, Y' = \text{CN}$ ) seem to stabilize the enols more than two  $\text{CO}_2\text{Me}$  groups both computationally and experimentally.<sup>2</sup> A small amount of enol was observed when  $Y = \text{CO}_2\text{Me}$ ,  $Y' = \text{NO}_2$ ,<sup>2</sup> nitromalondiamide is an enol in the solid state,<sup>5a</sup> and few examples are known for enols of amides when  $Y, Y' = \text{CO}$  groups.<sup>5b-e</sup> Amide **5**, where  $Y = \text{CN}$ ,  $Y' = \text{CO}_2\text{Me}$ , and  $\text{Ar} = \text{Ph}$  exist as the enol in the solid,<sup>2</sup> shows appreciable amounts of enol in solution and displays an exchange process (presumably  $\mathbf{1} \rightleftharpoons \mathbf{2}$ ) in solution.<sup>2</sup>



For a systematic study of the effect of  $\beta$ -substituents on the stabilization of the enols, we want to extend the study of systems **3/4** to other systems. There are five prerequisites: (i) higher  $K_{\text{Enol}}$  than for **3a/4a** which exist as the amide **4a** in the solid and ca. 5% of **3a** in  $\text{CDCl}_3$ , (ii) having at least one hydrogen bond acceptor group, Y and/or Y', (iii) an ability to increase the EW ability of Y, Y' without affecting much the steric hindrance in the system, (iv) one group (Y or Y') with a relatively low steric effect, and (v) Y, Y' groups which will not be the enolization sites, as shown, e.g., for a  $Y, Y' = \text{C}=\text{O}$  groups.<sup>1</sup> An ester group in a  $\text{C}_\beta(\text{CONHAr})\text{CO}_2\text{R}$  moiety is known to be a less prone enolization site than an amido group,<sup>1-3</sup> and the calculated  $K_{\text{Enol}}$  for  $\text{CH}_3\text{CO}_2\text{Me}$  is lower than that for  $\text{CH}_3\text{CONH}_2$ .<sup>4a</sup>

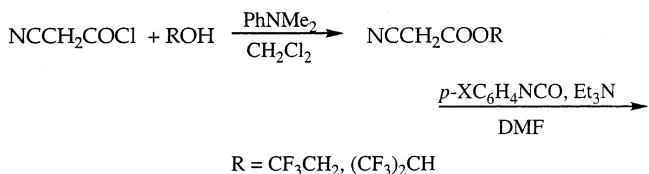
These requirements are fulfilled for the combination of  $Y = \text{CO}_2\text{R}$ ,  $Y' = \text{CN}$ . The cyano is a somewhat better electron-withdrawing group than an ester group, and the evidence above indicates that it enhances more the enol formation. Its linearity leads to relatively low steric demand, and it does not compete with CONHAr as an enolization site. The single ester group will enable hydrogen bonding stabilization of the enol, and modification of its EWG properties by fluorine substitution at its alkyl group will enable comparison with the known enol of amide **5**.<sup>2</sup>

We hoped that these CN,  $\text{CO}_2\text{R}$  substituted systems will extend the range in which the enols were observed to solvents more polar than  $\text{CDCl}_3$ . However, the apparent increased acidity may lead to complete ionization of  $\text{RO}_2\text{CCH(CN)CONHAr}$  in solution. We therefore prepared and studied several such systems.

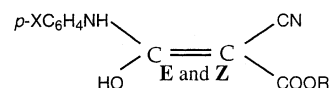
(5) (a) Simonsen, O.; Thorup, N. *Acta Crystallogr., Sect. B: Struct. Sci.* **1979**, *35*, 432. (b) Carrondo, M. A. A. F. de C. T.; Matias, P. M.; Heggie, W.; Page, P. R. *Struct. Chem.* **1994**, *5*, 73. (c) Bordner, J. *Acta Crystallogr., Sect. B: Struct. Sci.* **1979**, *35*, 215. (d) Glatz, B.; Helmchen, G.; Muxfeldt, H.; Porcher, H.; Premo, R.; Senn, J.; Stezowski, J. J.; Stojda, R. J.; White, D. R. *J. Am. Chem. Soc.* **1971**, *101*, 2171. (e) Mukhopadhyaya, J. K.; Rappoport, Z. Unpublished results.

## Results

**Synthesis.** Reaction of cyanoacetyl chloride with 2,2,2-trifluoroethanol or 1,1,1,3,3,3-hexafluoroisopropanol in  $\text{CH}_2\text{Cl}_2$  in the presence of *N,N*-dimethylaniline gave 2,2,2-trifluoroethyl or 1,1,1,3,3,3-hexafluoroisopropyl cyanoacetates. Their reaction with four *p*-X-substituted phenyl isocyanates ( $X = \text{H}, \text{MeO}, \text{Me}, \text{Br}$ ) in the presence of  $\text{Et}_3\text{N}$  in DMF gave eight compounds which a priori could be the amides (**6a-d**, **8a-d**) or their enols (**7a-d**, **9a-d**).



$p\text{-XC}_6\text{H}_4\text{NHCOCH(CN)COOR}$  and/or



<b>6a</b>	X = MeO	R = $\text{CF}_3\text{CH}_2$	<b>7a</b>
<b>6b</b>	X = Me	R = $\text{CF}_3\text{CH}_2$	<b>7b</b>
<b>6c</b>	X = H	R = $\text{CF}_3\text{CH}_2$	<b>7c</b>
<b>6d</b>	X = Br	R = $\text{CF}_3\text{CH}_2$	<b>7d</b>
<b>8a</b>	X = MeO	R = $(\text{CF}_3)_2\text{CH}$	<b>9a</b>
<b>8b</b>	X = Me	R = $(\text{CF}_3)_2\text{CH}$	<b>9b</b>
<b>8c</b>	X = H	R = $(\text{CF}_3)_2\text{CH}$	<b>9c</b>
<b>8d</b>	X = Br	R = $(\text{CF}_3)_2\text{CH}$	<b>9d</b>
<b>5</b>	X = H	R = Me	<b>10</b>

Amide **5** and enol **10** were prepared similarly earlier.<sup>2</sup>

**Solid-State Structures.** The solid-state structures of two compounds, representatives of the trifluoro **6/7** and the hexafluoro **8/9** series were determined by X-ray diffraction and found to be the enols **7a** and **9b**. In both, as well as in **10**,<sup>2</sup> the OH group is cis to and, according to the O...O nonbonding distances, is intramolecularly hydrogen bonded to the ester group. The NH group is intermolecularly hydrogen bonded to a CN group of another molecule. The ORTEP drawing of **9b** is shown in Figure 1, and its stereoview is in Figure S1; the ORTEP drawing and stereoview of **7a** are given in Figures S2 and S3 of the Supporting Information. Selected bond lengths and angles are given in Table 1. General crystallographic information, all bond lengths and angles and position and thermal parameters for **9b** and **7a** are given in Tables S1–S10 in the Supporting Information.

The following features are important: (i) the C(1)–C(2) bonds of  $1.410 \pm 0.002 \text{ \AA}$  are very long for a C=C bond; (ii) the C(1)–O(1) bond of  $1.31 \text{ \AA}$  is a single bond; (iii) the C(1)–N(1) bond length of  $1.31\text{--}1.32 \text{ \AA}$  has a strong C=N bond character, (iv) the C(2)–C(3) and C(2)–C(6) bond of  $1.41\text{--}1.42 \text{ \AA}$  are short for  $\text{C}_{\text{sp}^2}\text{--C}_{\text{sp}^2}$  or  $\text{C}_{\text{sp}^2}\text{--C}_{\text{sp}}$  bonds, (v) the O(1)–O(2) nonbonded distances of  $2.51\text{--}2.54 \text{ \AA}$  indicate a strong asymmetric  $\text{ROC}=\text{O}\cdots\text{OH}$  hydrogen bond; (vi) the intermolecular N1'–N2 nonbonded distance of  $2.94\text{--}2.99 \text{ \AA}$  indicates an NHN hydrogen bond, which is weaker than the OHO bond; (vii) bond angles around the C(1)–C(2) bond are close to  $120^\circ$ , with the O(1)–C(1)–N(1) angle of  $116.6\text{--}116.9^\circ$  being the smallest; (viii) the twist angle of the double bond is small (e.g.,  $2.3^\circ$  for **7a**).

TABLE 1. Selected Bond Lengths (Å) and Angles (deg) for 7b and 9a at rt

bond	7b	9a <sup>a</sup>	angle	7b	9a <sup>a</sup>
C(1)C(2)	1.412 (5)	1.408(5)	O(1)C(1)N(1)	116.9(3)	116.6(3)
C(1)O(1)	1.308(4)	1.314(5)	O(1)C(1)C(2)	120. (3)	120.0(3)
C(1)N(1)	1.313(5)	1.321 (4)	N(1)C(1)C(2)	122.5(3)	123.4(3)
C(2)C(3)	1.415(5)	1.422(4)	C(3)C(2)C(6)	119.8(3)	120.9(3)
C(2)C(6)	1.417(5)	1.408(4)	C(3)C(2)C(1)	119.3(3)	118.4(3)
C(3)O(3)	1.351(5)	1.357(4)	C(1)C(2)C(6)	120.9(3)	120.7(3)
C(4)O(3)	1.423(5)	1.424(4)	C(1)N(1)C(7)	124.9(3)	126.9(3)
C(3)O(2)	1.226(5)	1.227(4)	O(1)HO(2)	137.7	155.7
C(6)N(2)	1.131(5)	1.141(4)	N(1)HN(2) <sup>b</sup>	154.9	150.8
C(7)N(1)	1.435(4)	1.431(4)			
Ar	1.368(5)–1.399(5)	1.367(5)–1.377(5)			
O(1)H	1.18	1.12			
N(1)H	0.99	0.99			
O(2)···HO(1)	1.54	1.45			
N(2)···HN(1')	2.01	2.08			
O(1)O(2) <sup>c</sup>	2.54	2.51			
N(1)N(2) <sup>c</sup>	2.94	2.99			

<sup>a</sup> The bond lengths and bond angles of a second crystallographically different molecule differ by 0–0.008 Å and 0.2–1.0°, respectively. <sup>b</sup> Intermolecular bond lengths. <sup>c</sup> Nonbonded distances.

TABLE 2. Solid-State <sup>13</sup>C CP-MAS Spectra (δ in ppm) of Systems 6/7 and 8/9<sup>a</sup>

compound	C <sub>α</sub> <sup>a</sup>	COO	CF <sub>3</sub>	CN	CH/CH <sub>2</sub>	C <sub>β</sub> <sup>a</sup>	C–X <sup>b</sup>	C–N	C <sub>o,m</sub>	X <sup>b</sup>
6a/7a	171.6	171.6	ca. 126	118.1	60.7	57.1	159.6	126.4	126.4	54.5
6b/7b	171.5	171.5	ca. 126	117.5	60.4	57.2	136.3, 137.2	129.8, 131.2	ca. 125.3, ca. 126.0	19.7, 20.4
6c/7c	171.7	171.7	ca. 126	<i>c</i>	66.3	57.5		133.6	125.8, 128.7	
6d/7d	171.9	171.9	124.7	<i>c</i>	63.6	57.3, 58.5 <sup>d</sup>			133.1, 124.8	
8a/9a	173.1	169.7		114.7	66.7	56.9	159.0	129.8		53.2
8b/9b	170.8	170.8	ca. 126	<i>c</i>	65.7	56.7, 57.8	135.0	132.1	129.2, 129.2	20.1
8c/9c	172.6	170.3	ca. 128	117.0	65.6	57.0		132.5	128.1, 128.1	
8d/9d	171.6	170.4	126.7	115.1	65.1	57.4, 58.3	124.5	134.8	132.0	

<sup>a</sup> The δ values measured in the CP-MAS traces were confirmed to belong to quaternary carbons by the CP-NQS sequence. <sup>b</sup> X = *p*-substituent in the Ar group. <sup>c</sup> The δ values are not given, since either the signals are not observed or they are too broad and overlap a neighboring signal. <sup>d</sup> The two signals are probably due to the presence of two molecules in the asymmetric unit.

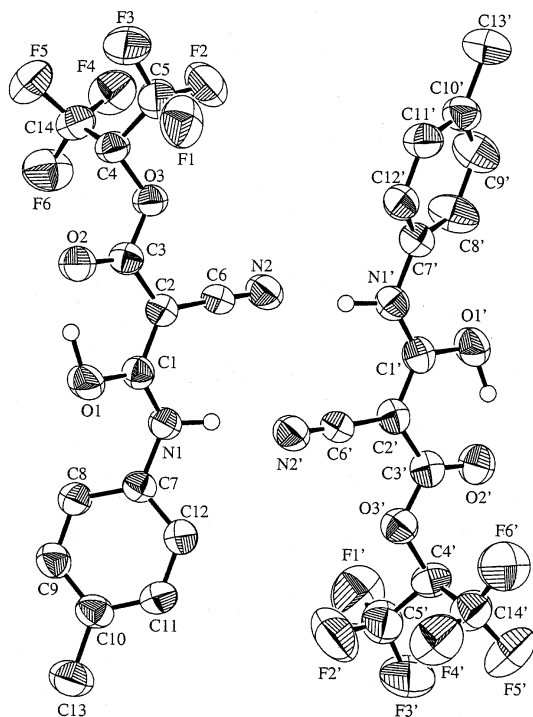


FIGURE 1. ORTEP drawing of 9b.

**Solid-State <sup>13</sup>C NMR Spectra.** A change of the aryl-ring substituents did not change the solid-state structure of several compounds **3**.<sup>3</sup> Since the structures of **7a**, **9b**,

and **10** are similar, we expect the other six compounds to also be enolic. This was corroborated by the solid-state <sup>13</sup>C NMR spectra of the eight systems (Table 2). In system **3**, the correspondence between the solid-state <sup>13</sup>C spectra and the solution <sup>13</sup>C spectra in cases where X-ray diffraction data were available enabled assignment of the solid-state structure. In the present case, we wondered if the intermolecular NH···NC hydrogen bond in the solid affected the <sup>13</sup>C shifts, whereas such strong interaction is absent in solution, as judged by the lack of concentration effect on the δ <sup>13</sup>C values (see below).

Broadening of signals in the solid state results in the overlap of neighboring signals, especially the CF<sub>3</sub> (which is sometimes 10 ppm broad) and CN signals (few of which have a very low intensity). However, comparison of the solid-state cross-polarization/magic-angle spinning (CP-MAS) δ <sup>13</sup>C values for C<sub>α</sub>, C<sub>β</sub>, and COO, where the errors are ±0.5 ppm with δ <sup>13</sup>C in THF-*d*<sub>8</sub> or CD<sub>3</sub>CN solution for all compounds (Table 4) show remarkable similarity, indicating an enol structure for all the substrates in the solid. This was further corroborated by the cross-polarization/nonquaternary suppression (CP-NQS) spectrum<sup>6</sup> which unequivocally identifies quaternary carbons by nullifying the hydrogenated carbons' signals. All the signals at δ 56.7–58.5 show that no hydrogen is attached to C<sub>β</sub>, thus excluding the amide structure (Table 2).

The differences Δδ<sub>α,β</sub> = δC<sub>α</sub> – δC<sub>β</sub>, are also character-

(6) Harris, R. K.; Kenwright, A. M.; Packer, K. J. *Magn. Reson. Chem.* **1985**, *123*, 216. Opella, S. J.; Frey, M. H. *J. Am. Chem. Soc.* **1979**, *101*, 5854.

TABLE 3.  $\delta(\text{OH})$  and  $\delta(\text{NH})$  Values (ppm) for *Z*-Enols and *E*-Enols<sup>a</sup>

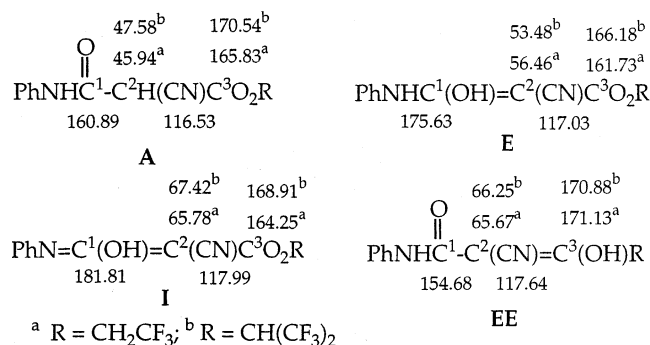
comp	solvent	<i>T</i> , K	$\delta(\text{OH})$		$\Delta\delta(\text{OH})^b$	$\delta(\text{NH})$		$\Delta\delta(\text{NH})^b$	$\Delta(\delta(\text{OH}) - \delta(\text{NH}))$		
			<i>Z</i> -enol	<i>E</i> -enol		<i>Z</i> -enol	<i>E</i> -enol		<i>Z</i> -enol	<i>E</i> -enol	
<b>7a</b>	CDCl <sub>3</sub>	298	<b>14.27</b>			<b>7.88</b>			<b>6.39</b>		
<b>7b</b>		298	<b>14.37</b>			<b>7.78</b>			<b>6.59</b>		
<b>7c</b>		298	<b>14.37</b>			<b>7.80</b>			<b>6.57</b>		
<b>7d</b>		298	<b>14.49</b>			<b>7.88</b>			<b>6.61</b>		
<b>9a</b>	THF- <i>d</i> <sub>8</sub>	298	<b>13.56</b>			<b>8.22</b>			<b>5.34</b>		
<b>9b</b>		240	13.60			8.82	10.49	-1.67	4.78		
		298	<b>13.65</b>			<b>8.18</b>			<b>5.47</b>		
<b>9c</b>		240	13.63			8.68	10.57	-1.89	4.95		
		298	13.67			8.33	10.63	-2.30	5.34		
<b>9d</b>		240	13.74			8.69	10.55	-1.86	5.05		
		298	13.68			8.39	10.62	-2.23	5.29		
<b>7a</b>		240	13.78			8.76	10.62	-1.86	5.02		
		298	14.00			9.61	10.78	-1.17	4.39		
		240	14.31			9.94	10.79	-0.85	4.37		
<b>7b</b>		220	14.31	11.39	2.92	10.03	10.77	-0.74	4.28	0.59	
		298	13.89			9.95	10.86	-0.91	3.94		
	240	14.40			10.01	10.96	-0.95	4.39			
<b>7c</b>	298				9.68	10.89	-1.31				
	280				9.80	10.90	1.10				
	260	14.42	11.09	3.33	9.91	10.93	-1.02	4.51	0.16		
<b>7d</b>	240	14.47	11.24	3.23	10.03	10.95	-0.92	4.44	0.29		
	220	14.48	11.38	3.10	10.15	10.96	-0.81	4.33	0.42		
	200	14.47	11.52	2.95	10.26	10.96	-0.70	4.21	0.56		
<b>9a</b>	298				9.73	10.89	-1.16				
	280				9.82	10.91	-1.09				
	260		11.04		9.95	10.92	-0.97				
<b>9b</b>	240	14.50	11.23	3.27	10.06	10.93	-0.87	4.44	0.30		
	220	14.51	11.37	3.14	10.16	10.94	-0.78	4.35	0.43		
	200	14.49	11.51	2.98	10.27	10.94	-0.67	4.22	0.57		
<b>9c</b>	298				<b>10.19</b>						
	200	13.25	11.01	2.24	10.42	10.52	-0.10	2.83	0.49		
	298	11.88			10.08			1.80			
<b>9d</b>	240	13.42	11.35	2.07	10.22	10.63	-0.41	3.20	0.72		
	200	13.33	11.26	2.07	10.41	10.64	-0.23	2.92	0.62		
	298	<b>11.50</b>			<b>10.12</b>			<b>1.38</b>			
<b>9c</b>	240	13.50	11.28	2.22	10.30	10.68	-0.38	3.20	0.60		
	298	<b>11.62</b>			<b>10.08</b>			<b>1.54</b>			
	240	13.24	11.73	1.51	10.31	10.66	-0.35	2.93	1.07		
<b>7a</b>	CD <sub>3</sub> CN	298	<b>14.04</b>			<b>8.42</b>			<b>5.62</b>		
		<b>7b</b>	298	<b>14.09</b>			<b>8.45</b>			<b>5.64</b>	
		<b>7c</b>	298	<b>14.04</b>			<b>8.52</b>			<b>5.52</b>	
<b>7d</b>		298	<b>14.28</b>			<b>8.50</b>			<b>5.78</b>		
<b>9a</b>		298	13.18			8.64	10.22	-1.58	4.54		
		240	13.07			8.81	10.19	-1.36	4.26		
<b>9b</b>		298	13.19			8.68	10.30	-1.62	4.51		
		240	13.12			8.85	10.28	-1.43	4.27		
<b>9c</b>		298	13.27			8.76	10.30	-1.54	4.53		
		240	13.18			8.91	10.34	-1.43	4.27		
<b>9d</b>		298	13.31			8.73	10.29	-1.56	4.58		
		240	13.38			8.88	10.28	-1.40	4.50		

<sup>a</sup> Bold numbers are for conditions when only one enol was observed. <sup>b</sup> The difference of the shifts between *Z*-enol and *E*-enol.

istic. They are 113.4–116.2 ppm, whereas the value for the amide PhNHCOCH(CONH<sub>2</sub>)<sub>2</sub> (106.9) is lower. However, this comparison involves an assumption that  $\Delta\delta_{\alpha,\beta}$  for **1** and **2** is independent of Y and Y'.

The shifts in the solid state were estimated by the ACD-LAB additivity scheme for C<sub>α</sub>, C<sub>β</sub>, COO, and CN of four isomers which should be considered in a complete analysis: the amide (A), the enol (E), the imine-ol (I), and the enol on the ester group (EE) (Chart 1). Despite the approximations of the scheme, comparison with the experimental  $\delta^{13}\text{C}$  values of C<sup>1</sup> and C<sup>3</sup> at 171.5–171.9 for **6/7** and 170.8–173.1 for **8/9** and of C<sup>2</sup> = 57.1–58.5 for **6/7** and 56.7–58.3 for **8/9**, exclude the imine-ol (too high C<sub>1</sub>), the enol on the ester (too low C<sub>1</sub>), and the amide (too low C<sub>1</sub> and C<sub>2</sub>) structures.

**Structure in Solution.** <sup>1</sup>H, <sup>13</sup>C, and <sup>19</sup>F NMR spectra were recorded for all systems in several solvents at several temperatures. Selected <sup>1</sup>H, <sup>13</sup>C, and <sup>19</sup>F NMR parameters are given in Tables 3–5, respectively, and

CHART 1. Estimated  $\delta^{13}\text{C}$  Values

the complete NMR parameters are given in Tables S11–S13 of the Supporting Information. There are several species in solution, and their structure, substituent, solvent, and temperature-dependent distribution was investigated.

TABLE 4.  $^{13}\text{C}$  NMR data for 6/7 and 8/9 systems in various solvents<sup>a</sup>

comp.	solvent	T (K)	COO	CON or C $_{\alpha}$	CN	CH or C $_{\beta}$
<b>9a-d</b>	CDCl <sub>3</sub>	298	169.05–169.16	170.57–170.70	114.02–114.44	57.34–57.69
<b>6a-d</b>	THF- <i>d</i> <sub>8</sub>	240	162.09–162.33	157.59–158.35	113.33–114.26	46.88–47.39
		298	162.03–162.24	157.69–158.15	112.98–113.11	46.96–47.03
<b>Z-7a-d</b>		240	171.53–171.62	172.57–172.66	114.44–114.82	57.66–58.56
		298	171.90–171.98	172.64–172.74	114.19–114.58	58.00–58.87
<b>E-7a-d</b>		240	168.67–168.91	168.05–168.24	116.19–116.53	59.17–60.10
		298	168.92–169.06	168.30–168.40	116.04–117.99	59.80–60.61
<b>Z-9a-d</b>		200	168.95–169.47	170.99–171.02	114.30–114.43	57.40–57.72
		240	169.06–169.23	171.30–171.41	113.82–114.00	57.93–58.44
		298	170.01	170.69–171.36	113.82–114.60	58.52–59.17
<b>E-9a-d</b>		200	165.80–166.04	169.35–169.56	116.00–117.55	58.78–58.88
		240	165.96–166.13	169.78–169.95	115.60–115.66	59.14–59.60
<b>6a-d</b>	CD <sub>3</sub> CN	298	161.26–161.33	157.18–157.21	112.55–112.67	46.58–47.34
<b>Z-7a-d</b>		298	171.10–171.17	171.41–171.46	114.15–114.60	56.99–57.45
<b>Z-9a-d</b>		240	168.40–168.46	170.18–170.26	113.48–113.76	56.61–57.21
		298	168.51–169.05	170.85–170.89	113.60–113.94	57.19–57.89
<b>6/7a-d</b>	DMSO- <i>d</i> <sub>6</sub>	298	166.98–167.74	166.25–166.43	120.00–121.19	57.53–59.23
<b>8/9a-d</b>		298	165.46–165.76	165.58–166.02	120.43–120.76	59.09–59.74
<b>6/7a,c</b>	DMF- <i>d</i> <sub>7</sub>	220	168.83, 169.13	168.80, 168.20	121.75, 122.71	59.84, 60.50
<b>6a</b>		220	158.37	157.23	121.60	
<b>6/7b,d</b>		240	168.70, 169.01	168.05	121.45, 122.22	60.02, 60.40
<b>6/7a-d</b>		298	168.16–169.17	167.73–168.38	120.72–121.90	59.53–59.80
<b>8/9a-d</b>		220	166.55–166.82	167.10–167.30	121.64–121.98	59.99–60.66
		298	166.38–166.65	167.05–167.89	119.75–120.80	59.48–60.40

<sup>a</sup> Signals for **8a-d** are too weak to be observed in THF-*d*<sub>8</sub>.

TABLE 5. Selected  $^{19}\text{F}$  Chemical Shift (ppm) for Compounds 6–9

comp	solvent	T, K	Z-enol	E-enol	amide	ion
<b>6a-d/7a-d</b>	CDCl <sub>3</sub>	298	-74.57 ± 0.01			
<b>8a-d/9a-d</b>	CDCl <sub>3</sub>	240	-73.82 ± 0.02	-73.94 ± 0.01		
<b>8a-c/9a-c</b>		298	-74.04 ± 0.02			
<b>6a-d/7a-d</b>	THF- <i>d</i> <sub>8</sub>	240	-74.55 ± 0.01	-75.50 ± 0.02	-75.21	
					-75.32	
		298	-75.57 to -75.65	-75.27 to -75.36	-75.28 to -75.35	
<b>8a-d/9a-d</b>		200	-76.89			
		240	-76.98 ± 0.01			
		298	-76.98 ± 0.01		-76.55	
<b>6a-d/7a-d</b>	CD <sub>3</sub> CN	298	-75.44 ± 0.01		-75.22 ± 0.01	
<b>8a-d/9a-d</b>		240	-75.01 ± 0.01	-75.03 ± 0.01		
		298	-74.98 ± 0.02			
<b>6a-d/7a-d</b>	DMSO- <i>d</i> <sub>6</sub>	298				-73.32 ± 0.01
<b>8a-d/9a-d</b>		298				-73.36 to -73.44
<b>6a-d/7a-d</b>	DMF- <i>d</i> <sub>7</sub>	220			-74.44	-74.64
		240			-74.43 to -74.64	-74.64 to -74.83
		298				-74.45 to -74.60
<b>8a-d/9a-d</b>		220				-74.41 to -74.54
		298				-74.35 to -74.54

In CDCl<sub>3</sub>. The  $^1\text{H}$  NMR spectra at 298 K differ for **6/7** and **8/9**. The trifluoroesters **7** display signals for only one species: a broad OH signal at  $\delta$  14.27–14.49, one NH singlet at  $\delta$  7.78–7.88 (Table 3), aryl and CH<sub>2</sub> signals at  $\delta$  6.92–7.53 and 4.62–4.63, respectively, and *p*-MeO ( $\delta$  3.83) and *p*-Me ( $\delta$  2.36) signals. No C–H signals of an amide were observed. The  $^{19}\text{F}$  NMR spectra show only one signal (Table 5). Due to the low solubility  $^{13}\text{C}$  NMR spectra at rt or  $^1\text{H}$  and  $^{19}\text{F}$  spectra at lower temperatures were not measured.

The hexafluoroesters **9** display at 298 K the OH, NH, Ar, and CH signals at  $\delta$  13.58–13.68 (br, 0.80–0.88H), 8.18–8.38, 6.93–7.54, and 5.82–5.83, respectively. The OH signal for **9d** is barely observed. All the compounds show a new 0.05–0.1H singlet at  $\delta$  10.5–10.6 (Table 3), and additional small signals overlap the main Ar signals.

At 240 K the lower field OH signal sharpened to a 1H signal for **9a-d**. The NH signal shifted downfield by 0.4–0.7 ppm, but the 0.09–0.11H signal did not shift. New MeO and Me signals with ca. 10% intensity appear for **9a** and **9b** at ca. 0.01 ppm upfield of the main MeO and Me signals. The new and old aromatic signals overlapped. The  $^{19}\text{F}$  NMR spectra display two signals at  $\delta$  ca. -73.8 and -73.9 in a 1.0:0.08 ratio at 240 K (Table 5), with minor differences at 298 K. The  $^{13}\text{C}$  NMR spectra at 298 K display signals at  $\delta$  ca. 170.6 (C $_{\omega}$ ), 169.1 (COO), 120.3 (CF<sub>3</sub>), 114.2 (CN), 114.5–151 (Ar), 66.8 (CH(CF<sub>3</sub>)<sub>2</sub>), 57.5 (C $_{\beta}$ , no C–H coupling), and 55.40 (MeO of **9a**) or 20.94 (Me of **9b**) (Tables 4 and S12). The data are consistent with the formation of two enols at an ca. 10:1 ratio. Evidence that they are the *Z*- and *E*-enols is given below.

**TABLE 6.**  $^1\text{H}$  and  $^{13}\text{C}$  NMR Chemical Shifts for the Species Formed from **9c** and  $\text{Et}_3\text{N}$  in  $\text{THF}-d_8$  at 240 K

hydrogen	$\delta$ $^1\text{H}$ , ppm ( $J$ , Hz) <sup>a</sup>	$\Delta\delta^1\text{H}$ , ppm <sup>a</sup>	carbon	$\delta$ $^{13}\text{C}$ , ppm ( $J$ , Hz)	$\Delta\delta^{13}\text{C}$ , ppm <sup>a</sup>
NH	10.48	0.18	$\text{C}_\alpha$	169.33 (d, $J = 5$ )	-2.08
acidic H	9.11		COO	166.73	-2.47
Ph-H	7.59 (d, $J = 7.9$ )		$\text{C}_{\text{ipso}}$	140.51 (t, $J = 9.6$ )	4.66
Ph-H	7.29 (t, $J = 7.8$ )		$\text{C}_o$	129.52 (dd, $J_1 = 158$ , $J_2 = 8.4$ )	-0.3
Ph-H	7.01 (t, $J = 7.4$ )		$\text{C}_p$	123.29 (dt, $J_d = 159$ , $J_t = 7.5$ )	-4.55
$\text{CH}(\text{CF}_3)_2$	6.46 (hep, $J = 6.5$ ) <sup>b</sup>	-0.29	$\text{C}_m$	120.03 (d, $J = 151$ )	-5.51
			$\text{CF}_3$	122.56 (q, $J = 282$ )	0.65
			CN	121.66	7.74
			$\text{CH}(\text{CF}_3)_2$	65.07 (d of hep, $J_d = 149$ , $J_{\text{hep}} = 33$ ) <sup>b</sup>	-1.69
			$\text{C}_\beta$	60.40	2.26

<sup>a</sup>  $\Delta\delta^1\text{H} = \delta(\text{enol}/\text{Et}_3\text{N}) - \delta(\text{Z-enol})$  for the same hydrogen;  $\Delta\delta^{13}\text{C} = \delta(\text{enol}/\text{Et}_3\text{N}) - \delta(\text{Z-enol})$  for the same carbon. <sup>b</sup> hep = heptet.

**In THF.** In THF, signals for three species (*Z*-enol, *E*-enol and amide) are observed at both 298 and 240 K. For compounds **6/7** at 298 K, the lowest field signal in the  $^1\text{H}$  NMR spectrum (OH of **Z-7**) is very broad at  $\delta$  13.89–14.00 (<1H) for **7a** and **7b** and not observed for **7c** and **7d**. However, at 240 K, it somewhat sharpens, appearing at  $\delta$  ca. 14.4 for **7a–d**, and it shifts systematically to a lower field on increased electron withdrawal. The 1H NH signals at  $\delta$  9.60–9.74 at 298 K shift to 9.91–10.08 at 240 K (Table 3). The  $\delta(\text{OH}, \text{E-7})$  is at  $\delta$  10.73–10.90 (10.79–10.96) at 298 (240) K with 0.2–0.3 intensity of  $\delta(\text{OH}, \text{Z-7})$ . For the amides **6a–d** a broad CH singlet is observed at  $\delta$  5.02–5.05 (298 K) and 5.08–5.12 (240 K) with 0.13–0.17 intensity of the NH of **Z-7**. The amide NH at 298 K overlaps the **Z-7** OH signal but is observed at 240 K at  $\delta$  9.99–10.24. Three MeO or Me signals for **6a/7a** and **6b/7b** were observed (Table S11). The broad  $\text{CH}_2$  quartets at 298 K separate at 240 K to two sharper quartets with, e.g., 1.0:0.2 ratio for **6a/7a**. The aromatic signals for the three species overlap. The  $^{19}\text{F}$  NMR at 240 K show three signals (Table S13).

The  $^{13}\text{C}$  NMR spectra (Table 4) also show signals for three species. The lower field CO and  $\text{C}_\alpha$ , the CN, and the upper field  $\text{C}_\beta$  are well separated. E.g., at 240 K,  $\delta$  is at ca. 172.6 (COO), 171.5 ( $\text{C}_\alpha$ ), 114.6 (CN), 57.7–58.6 ( $\text{C}_\beta$ ) for *Z*-enol, 168.8 (COO), 168.3 ( $\text{C}_\alpha$ ), 116.4 (CN), 59.2–60.1 ( $\text{C}_\beta$ ) for the *E*-enol, and 162.2 (COO),  $157.9 \pm 0.4$  ( $\text{C}_\alpha$ ),  $114.0 \pm 0.7$  (CN), and 46.9–47.4 (d,  $J = 138$  Hz,  $\text{C}_\beta\text{H}$ ) for the amide.

Systems **8/9** display, in the  $^1\text{H}$  NMR spectrum, two very broad lowest field signals at  $\delta$  10.2–13 and 8.8–10.2 at 298 K but five broad signals at  $\delta$  ca. 13.4, 11.9, 10.6, 10.25, and 10.2 at 240 K. The signals do not overlap at 180 and 200 K, but at 260 K the first three signals merge (Table 3). At 200 K, most of the signals are sharp, except for a few of the two  $\text{CH}(\text{CF}_3)_2$  heptets. The  $^{19}\text{F}$  NMR spectra at 240 K show one signal.

The  $^{13}\text{C}$  NMR spectra at 298 K indicate that a dynamic process takes place. The COO and  $\text{C}_\alpha$  signals display a broad signal centered at 171 ppm, whereas at 200 or 240 K, sharp signals are consistent with the presence of two enols.  $\text{C}_\alpha$  and  $\text{C}_\beta$  are at 171.0–171.4 and 57.4–58.4 for **Z-9** and at 169.4 and 58.8–59.6 for **E-9**.  $\Delta\delta_{\text{C}_\alpha, \text{C}_\beta}$  ca. 111–113. (Other signals are in Tables 4 and S12.) Low intensity amide signals appear for **8d/9d**.

When a drop of  $\text{D}_2\text{O}$  was added at 298 K, the broad signals shifted only slightly. However, at 200 K, the  $\text{C}_\alpha$ , CN,  $\text{C}_{\text{ipso}}-\text{MeO}$ , and  $\text{C}_\beta$  signals of the two enols split to two signals due to isotope-induced shifts due to isotopomeric O–H, O–D, N–H, and N–D species. In an attempt

to distinguish the new signals from those in the nondeuterated species, 3  $\mu\text{L}$  of  $\text{H}_2\text{O}$  or  $\text{D}_2\text{O}$  was added separately to 0.5 mL of  $\text{THF}-d_8$  containing **9a**. For nonsplit signals, this resulted in similar  $\delta^{13}\text{C}$  shifts. The assumption that this applies for all the signals led to only one unequivocal assignment: the new signals of  $\text{C}_\alpha$  are at 10 and 12 Hz up field from the signals for the nonlabeled *Z*- and *E*-enols.  $\text{C}_{\text{ipso}}-\text{MeO}$ , CN, and  $\text{C}_\beta$  of **E-9a** display splittings of 6, 6, and 3 Hz, respectively, and the CN of **Z-9a** displays a splitting of 10 Hz. Less safe assignments are the splitting of 5 and 22 Hz of the  $\text{C}_m$  signal of **Z**- and **E-9a**, respectively.

The addition of 3% (v/v) of  $\text{Et}_3\text{N}$  to the **8/9b,c** mixtures simplified the  $^1\text{H}$ ,  $^{13}\text{C}$ , and  $^{19}\text{F}$  spectra to that of a single compound. E.g., at 240 K (or 298 K) a 0.22M **8b/9b** mixture displayed  $^1\text{H}$  signals of NH, Ar–H,  $\text{CH}(\text{CF}_3)_2$ , and  $\text{CH}_3$  at  $\delta$  11.35, 7.41, 7.04, and 6.41,  $\text{Et}_3\text{N}$  signals at 1.05 and 2.69, a broad signal at 10.0, and a small (0.05H) signal at 11.30. For  $\text{Et}_3\text{N}$  alone  $\delta = 0.95$  and 2.41. In the  $^{13}\text{C}$  NMR spectrum  $\text{C}_\alpha$  and COO are shifted upfield 2 and 2.4 ppm, the Ar–C signals shift slightly, and the CN,  $\text{CF}_3$ , and  $\text{C}_\beta$  shift downfield by ca. 6, 0.6, and 2.3 ppm compared with the **Z-9b** signals. Similar spectra were observed from **8c/9c**, and the shifts for **9c** are given in Table 6. The  $^{19}\text{F}$  NMR shows only one signal.

There is no significant concentration dependence of the chemical shifts. At 200 K the  $\delta^{13}\text{C}$  values of the  $\text{C}_\alpha$ , COO, and  $\text{C}_\beta$  signals and  $\delta(^1\text{H})$  of the OH and NH signals of **Z-7c**, **E-7c**, and **6c** were identical within 0.04 ppm, respectively, at 0.07 and 0.56 M concentrations. The three  $^{13}\text{C}$  signals of **6d**, **Z-7d**, and **E-7d** differed by <0.08 ppm (except for two values differing by 0.13 and 0.15 ppm) at 0.055 and 0.18 M concentrations. This excludes an important intermolecular enol–enol association.

The *Z*-enol/*E*-enol equilibrium ratios and the  $K_{\text{Enol}}$  values were calculated from the integrations of the mostly sharp NH signals of the three species (Table 7). The integrations of the NH and CH of the amide were similar. When possible, the values were also calculated from the  $^{19}\text{F}$  NMR data and they resembled, within the experimental error, those based on  $^1\text{H}$  NMR.

The spectra of the diester **3d/4d** (Ar = *p*-MeOC<sub>6</sub>H<sub>4</sub>) were measured in  $\text{THF}-d_8$  at 298 K for comparison with that of **7a**. The signals for **3d** are at  $\delta$  16.02 (OH) and 11.34 (NH) and for **4d** at 9.28 (NH) and 4.83 (CH). The  $K_{\text{Enol}}$  is 0.4 (298 K) and 0.36 (240 K).

**In CD<sub>3</sub>CN.** The solubility of derivatives **6/7** at 240 K is low, and the spectra were measured only at 298 K, whereas for **8/9** they were recorded at both temperatures. For **6/7** at 298 K, a broad OH signal and a slightly broad

**TABLE 7.** Z-Enol, E-Enol, and Amide Composition and  $K_{\text{Enol}}$  in THF- $d_6$  at Several Temperatures

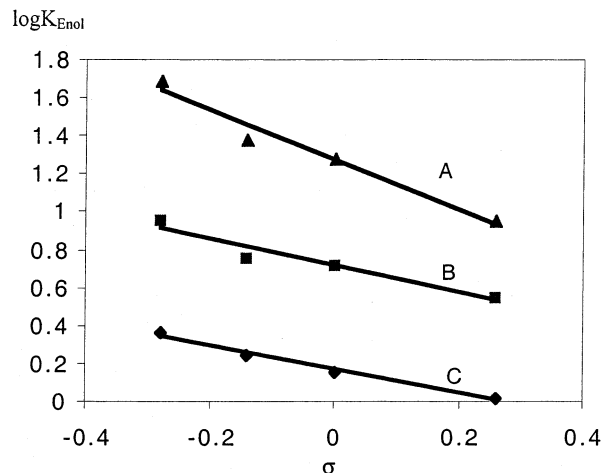
comp	T, K	% Z-enol	% E-enol	% amide	$K_{\text{Enol}}^a$	Z-enol/E-enol	NMR method <sup>b</sup>
<b>6a/7a</b>	180	75 (74)	21 (22)	4 (4)	24 (24)	3.6 (3.4)	<sup>1</sup> H ( <sup>19</sup> F)
	200	72 (72)	24 (24)	4 (4)	24 (24)	3.0 (3.0)	<sup>1</sup> H ( <sup>19</sup> F)
	240	77 (74)	18 (20)	5 (6)	19 (16)	4.3 (3.7)	<sup>1</sup> H ( <sup>19</sup> F)
	260	77 (76)	17 (18)	6 (6)	16 (16)	4.5 (4.2)	<sup>1</sup> H ( <sup>19</sup> F)
	280	82	11	7	13	7.5	<sup>19</sup> F
	300		91 <sup>c</sup>	9	10		<sup>19</sup> F
<b>6b/7b</b>	320	88 <sup>c</sup>	12	7		<sup>19</sup> F	
	240	70 (71)	20 (20)	10(9)	9(10)	3.5 (3.6)	<sup>1</sup> H ( <sup>19</sup> F)
	298	70 (87 <sup>g</sup> )	16	12(13)	7 (7)	4.4	<sup>1</sup> H ( <sup>19</sup> F)
<b>6c/7c</b>	200	68 (66)	21 (23)	11(11)	8 (8)	3.2 (2.9)	<sup>1</sup> H ( <sup>19</sup> F)
	220	69 (68)	19 (21)	12(11)	7 (8)	3.6 (3.2)	<sup>1</sup> H ( <sup>19</sup> F)
	240	68 (68)	19 (20)	13(12)	7(7)	3.6 (3.4)	<sup>1</sup> H ( <sup>19</sup> F)
	260	68 (69)	18 (18)	14(13)	6 (7)	3.8 (3.8)	<sup>1</sup> H ( <sup>19</sup> F)
	280	69	17	14	6	4.1	<sup>19</sup> F
	300		84 <sup>c</sup>	16	5		<sup>19</sup> F
<b>6d/7d</b>	200	64 (59)	23 (28)	13(13)	7(6)	2.8 (2.1)	<sup>1</sup> H ( <sup>19</sup> F)
	220	65 (63)	21 (22)	14(15)	6 (6)	3.1 (2.9)	<sup>1</sup> H ( <sup>19</sup> F)
	240	66 (65)	20 (20)	14(15)	6 (6)	3.3 (3.2)	<sup>1</sup> H ( <sup>19</sup> F)
	260	63 (65)	22 (18)	15(17)	6(5)	2.9 (3.6)	<sup>1</sup> H ( <sup>19</sup> F)
	280	64 (65)	18 (17)	18(18)	5(5)	3.6 (3.8)	<sup>1</sup> H ( <sup>19</sup> F)
	300		80 <sup>c</sup>	20	5		<sup>19</sup> F
<b>8a/9a</b>	320	68 <sup>c</sup>	32	3		<sup>19</sup> F	
	330	62 <sup>c</sup>	38	2		<sup>19</sup> F	
	180	38	62		$\geq 100^d$	0.61	<sup>1</sup> H
	200	44	56		$\geq 100^d$	0.79	<sup>1</sup> H
	220	50	50		$\geq 100^d$	1.0	<sup>1</sup> H
	240	56	44		$\geq 100^d$	1.27	<sup>1</sup> H
<b>8b/9b</b>	260	60	40		$\geq 100^d$	1.5	<sup>1</sup> H
	280	63	37		$\geq 100^d$	1.7	<sup>1</sup> H
	300		100 <sup>c</sup>		$\geq 100^d$		<sup>1</sup> H
	180	37.8	61.8	0.4	249	0.61	<sup>1</sup> H
	200	44.6	54.9	0.5	199	0.81	<sup>1</sup> H
	220	49.5	49.5	1.0	99	1.0	<sup>1</sup> H
<b>8c/9c</b>	240	53.5	45.5	1	99	1.18	<sup>1</sup> H
	260	54.6	43.2	2.2	44	1.26	<sup>1</sup> H
	280	62	38	<i>e</i>		1.63	<sup>1</sup> H
	300		100 <sup>c</sup>				<sup>1</sup> H
	240	50	48	2	49	1.04	<sup>1</sup> H
	298		100 <sup>c</sup>				<sup>1</sup> H
<b>8d/9d</b>	180	27	72	1	99	0.38	<sup>1</sup> H
	200	34	64.6	1.4	70	0.52	<sup>1</sup> H
	220	40	58	2	49	0.69	<sup>1</sup> H
	240	44.8	51.6	3.6	27	0.87	<sup>1</sup> H
	260	50.5	44.4	5.1	19	1.13	<sup>1</sup> H
	280	57.5	35.6	6.9	14	1.61	<sup>1</sup> H
<b>10</b>	300		90 <sup>c</sup>	10	9		<sup>1</sup> H
	320		85 <sup>c</sup>	15	6		<sup>1</sup> H
	180	67	5	28	3	13.2	<sup>1</sup> H
	200	68	4	28	3	17	<sup>1</sup> H
<b>10</b>	220	68	4	28	3	17.2	<sup>1</sup> H
	240	67	3	30	3	22.3	<sup>1</sup> H
	260	67	3	30	3	22.3	<sup>1</sup> H
	280	65	3	32	2	21.7	<sup>1</sup> H
	298	64	3	33	2	21.3	<sup>1</sup> H

<sup>a</sup>  $K_{\text{Enol}} = ([\text{E-enol}] + [\text{Z-enol}]) / [\text{Amide}]$ . <sup>b</sup> Integration of the signals for the three species. <sup>1</sup>H: integration of the NH signals in the <sup>1</sup>H NMR spectrum. <sup>19</sup>F: integration of the F signals in the <sup>19</sup>F NMR spectrum. <sup>c</sup> The signals of the two enols merge to one signal. <sup>d</sup> Assuming that 1% of the amide NH could have been observed. <sup>e</sup> Broad signal.

NH signal at  $\delta$  14.0–14.3 and  $\delta$  8.4–8.5 (Table 3) were ascribed to the enol. A slightly broad signal at  $\delta$  8.7–8.9 and a quartet at  $\delta$  4.92–4.97 with 1:1 ratio are due to the NH and CH of the amide. However, the presence of three species is evident by the overlapping aromatic signals and the three MeO signals of **6a/7a** at  $\delta$  3.80, 3.78, and 3.75 with an approximate 3.0:1.1:0.26 ratio. The <sup>19</sup>F NMR spectra (Table 5) display two signals. The <sup>13</sup>C NMR spectra (Table 4) display discrete signals for two species. E.g., for the enol at  $\delta$  ca. 171.45 (COO), 171.13

**TABLE 8.** Enols/Amide Compositions in CD<sub>3</sub>CN

comp	T, K	% Z-enol	% E-enol	% amide	$K_{\text{Enol}}^a$	Z-enol/E-enol
<b>6a/7a</b>	298	70		30	2.33	
<b>6b/7b</b>	298	64		36	1.78	
<b>6c/7c</b>	298	59		41	1.44	
<b>6d/7d</b>	298	51		49	1.04	
<b>8a/9a</b> <sup>a</sup>	298	80	10	10	9.00	8
<b>8b/9b</b>	298	77	8	15	5.67	9.6
<b>8c/9c</b>	298	72	12	16	5.25	6
<b>8d/9d</b>	298	66	12	22	3.54	5.5
<b>8a/9a</b>	240	85	13	2	49	6.5
<b>8b/9b</b>	240	85	11	4	24	7.7
<b>8c/9c</b>	240	85.5	9.5	5	19	9.0
<b>8d/9d</b>	240	78	12	10	9	6.5

**FIGURE 2.**  $\log K_{\text{Enol}}$  vs  $\sigma$  for  $p\text{-XC}_6\text{H}_4\text{NHC(OH)=C(CN)CO}_2\text{R}$  in CD<sub>3</sub>CN: (A) R = CH(CF<sub>3</sub>)<sub>2</sub> at 240 K; (B) R = CH(CF<sub>3</sub>)<sub>2</sub> at 298 K; (C) R = CH<sub>2</sub>CF<sub>3</sub> at 298 K.

(C<sub>α</sub>), and 57.2 (C<sub>β</sub>) and corresponding ones for the amide at 161.3, 157.2, and 46.58–47.37 (Table 4).

The **7/6** ratios were calculated from the intensities of the NH signals and increased from 2.2 for *p*-MeO (**6a/7a**) to 1.04 for *p*-Br (**6d/7d**) (Table 8). A  $\log K_{\text{Enol}}$  vs Hammett's  $\sigma$  values is linear with  $\rho = -0.64$  ( $R^2 = 0.9893$ , Figure 2). A plot vs  $\sigma^+$  is curved.

Systems **8/9** display signals for **Z-9**, **E-9**, and **8** at 298 and 240 K: at  $\delta$  ca. 13.2 (br OH), 8.7 (NH) in 1:1 ratio for **Z-9**, at 10.25 (NH) for **E-9**, and at ca. 8.9 (NH), 5.1 (CH) [1:1] for **8**. At 240 K, the <sup>1</sup>H signals are sharper. On shaking with D<sub>2</sub>O and immediate monitoring,  $\delta$ (OH) disappeared, and the NH and CH signals had lower intensities. The three signals in the <sup>19</sup>F NMR spectra are in ratios similar to those of the NH signals. The rt <sup>13</sup>C NMR spectra showed signals for only one enol, but at 240 K, signals for the three species were observed with C<sub>α</sub> at ca. 170.3 and C<sub>β</sub> at 56.5–57.9 ppm, i.e.,  $\Delta\delta_{\alpha,\beta}$  ca. 113 ppm. Addition of CF<sub>3</sub>COOH led to sharper signals.

$K_{\text{Enol}} = ([\text{Z-9}] + [\text{E-9}]) / [\text{8}]$  is higher for more electron donating aryls. It decreases at 298 K from 9.0 for **8a/9a** to 3.5 for **8d/9d**, and at 240 K from 49 to 9.0. Although the error in  $K_{\text{Enol}}$  is larger than that for **6/7**, Hammett's  $\log K_{\text{Enol}}$  vs  $\sigma$  plots are reasonably linear with  $\rho = -0.70$  ( $R^2 = 0.9316$ ) at 298 K and  $-1.23$  ( $R^2 = 0.968$ ) at 240 K (Figure 2). The Z-Enol/E-Enol ratios are not much substituent dependent (Table 8).

In DMF-*d*<sub>7</sub>. All compounds show similar spectral characteristics in DMF-*d*<sub>7</sub>. In the <sup>1</sup>H NMR spectrum at

298 K, there is a broad  $\leq 1\text{H}$  signal at  $\delta$  12.9–16.1, a slightly broad  $1\text{H}$  signal at 10.22–10.75, and  $\text{CH}_2$  or  $\text{CH}$  signals at ca.  $\delta$  4.85 and 6.4, respectively. At 240 K, the *p*-Me and *p*-MeO signals (Table S11) are singlets, frequently accompanied by  $\leq 5\%$  overlapping signals. Small (4–11%) signals are sometimes observed around  $\delta$  11.3–11.6 (NH) and 5.7 (CH) or overlap the main aromatic signals. At 240 K, the lower field signal (now a broadened ca.  $1\text{H}$ ) is further shifted to  $\delta$  14.9–17.2. Other signals become sharper. The  $^{19}\text{F}$  NMR spectrum at 298 or 220 K displays a major  $^{19}\text{F}$  signal accompanied by another low intensity signal.

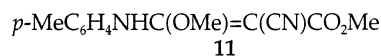
The  $^{13}\text{C}$  NMR spectra at 220 K show two broad carbonyl signals at  $\delta$  168.0–169.2 for **6/7** and at 166.4–167.3 for **8/9**, 4 Ar, CN (ca. 125.6) and  $\text{CF}_3$  (ca. 125.2) signals, a higher field  $\text{CH}_2\text{CF}_3$  (58.6–58.9) or  $\text{CH}(\text{CF}_3)_2$ , and a singlet at ca. 60 ppm uncoupled to an hydrogen ( $\text{C}_\beta$ ). Additional signals are consistent with small percent of the amide.

For **8/9** at 298 K, nonsharp signals for only one species were observed. At 220 K, they are at  $167.2 \pm 0.1$  ( $\text{C}_\alpha$ ),  $166.7 \pm 0.1$  (COO),  $122.5 \pm 0.1$  ( $\text{CF}_3$ ),  $121.8 \pm 0.2$  (CN), 65.1 ( $\text{CH}(\text{CF}_3)_2$ ), and  $60.3 \pm 0.3$  ( $\text{C}_\beta$ ). Few additional small signals are observed.

Significantly, on addition of three drops of aqueous 3 N NaOH solution or of  $\text{Et}_3\text{N}$  to **7a**, **9a**, **9b**, or **9d**, the  $^{13}\text{C}$  and the  $^{19}\text{F}$  spectra display only small shifts of the signals. In the  $^1\text{H}$  NMR spectrum, the signal at low field and at  $\delta$  5.7 for **7a** disappears. However, whereas the  $\delta(\text{OH})$  signal of the enols is only slightly temperature dependent, the broad low field signal in DMF shifts significantly, e.g., for **9b**, from 16.12 (rt) to 17.45 at 220 K, or from  $\delta$  13.98 (rt) to 15.55 (220 K) for **9c**. The corresponding  $\delta(\text{NH})$  values change by  $< 0.07$  ppm.

We ascribe the signal at  $\delta$  ca. 13–17 to the solvated proton and the other signals to the conjugate base of the species, both formed by ionization. The  $\delta$  of this proton should be concentration dependent if exchange with the neutral species takes place. If the anion is the main species in neutral solution, the added base ensures a complete ionization and reduces the rate of the exchange process. On the basis of the NH signals and assuming that the small NH signal is due to the amide, compounds **8a–d** and **9a–d** at 220 and 298 K and **6a–d** and **7a–d** at 298 K exist completely as the ion, whereas at 220 K, there are 6%, 10%, and 4% amide for **6a**, **6b**, and **6c**, respectively.

**Deuteration Experiments.** When the sample was shaken with  $\text{D}_2\text{O}$  and immediately monitored, the low field signal disappears completely and the signal at  $\delta$  ca. 10.5 is reduced to  $< 10\text{--}0\%$ . The extent of deuterium-induced shifts caused by N–D vs N–H on  $\text{C}_\alpha$  could not be evaluated for system **7**, since both the N–H and the residual O–H hydrogens are exchanged. No *N*-alkyl derivative of **7** is available, but we studied the changes in the  $^{13}\text{C}$  NMR spectra of the enol ether **11**<sup>7</sup> after



deuteration. On addition of 1:1  $\text{H}_2\text{O}/\text{D}_2\text{O}$  at 220 K to **11** in DMF- $d_7$ , the N–H signal was 45% deuteriated, and

$^{13}\text{C}$  signals at  $\delta$  169.35, 138.86, 130.77, 118.56, 62.60, 62.27, 52.56, and 21.05 were shifted without splitting to 169.07, 138.70, 130.58, 118.41, 62.39, 61.90, 52.41, and 20.82. The signals at  $\delta$  171.70 ( $\text{C}_\alpha$ ), 134.49 ( $\text{C}_{\text{ipso-N}}$ ), and 125.25 ( $\text{C}_\alpha$ ) split, and the new deuterium-induced signals were 0.11, 0.12, and 0.10 ppm (0.08, 0.10, and 0.08 ppm at 298 K) upfield. The COOMe carbon also shows 0.07 ppm splitting at 298 K.

When a sample of **7a** was exchanged with 1:1  $\text{H}_2\text{O}/\text{D}_2\text{O}$  in DMF- $d_7$ , the N–H group was 66% exchanged and the OH signal disappeared. At 220 K  $\text{C}_\alpha$ ,  $\text{C}_{\text{ipso-Ome}}$  and  $\text{C}_\alpha$  to N of **7a** split by 0.12, 0.06, and 0.20 ppm, respectively. In the 60% deuteriated amide, the COO and CN split by 0.11 and 0.13 ppm, respectively.

**In DMSO- $d_6$ .** The compounds are probably also ionized in DMSO- $d_6$ . In the  $^1\text{H}$  NMR spectra of **6/7**, there is no OH signal at a  $\delta$  value larger than  $\delta$  10.4, and only a broad NH signal is at 10.3–10.4. A broadened aromatic multiplet, a  $\text{CH}_2$  quartet, and a broad signal at 6.5–7.8 were observed. The  $^{13}\text{C}$  NMR spectra display signals at  $\delta$  167.0–167.7, 165.4–166.4, and 159.40 (for **6a/7a**) and 139.4 (for **6/7 c,d**), and a  $\text{CH}_2$  signal at  $\delta$  58.0–58.3. A singlet at  $\delta$  57.5–59.2 (probably  $\text{C}_\beta$ ) overlaps the  $\text{CH}_2$  signal (Tables 4 and S12). The  $^{19}\text{F}$  spectrum displays a signal at  $-73.3$ . Addition of NaOH to **7c** did not affect the  $^{13}\text{C}$  and  $^{19}\text{F}$  spectra, and two added drops of  $\text{CF}_3\text{-COOH}$  did not affect the  $^1\text{H}$ ,  $^{13}\text{C}$ , and  $^{19}\text{F}$  spectra.

For the **8/9** series, there are two broad  $^1\text{H}$  signals at  $\delta$  11.7–12.6 and 9.9–10.1 and aromatic,  $\text{CH}(\text{CF}_3)_2$ , and *p*-Me and *p*-MeO signals. On addition of a few drops of 3 N NaOH to **9b–9d**, the first, but not the second, signal disappeared, and addition of TFA to **8a/9a** shifted the lower field signal to  $\delta$  13.78. Other signals of 5–6% intensity appear in the aromatic region or in the *p*-Me region of **8b/9b**. In the  $^{19}\text{F}$  NMR spectra, a single signal is at  $\delta$   $-73.4$ . Addition of NaOH or TFA results in signals sharpening and only minor shifts in the  $^{13}\text{C}$  NMR spectra to signals at  $\delta$  ca. 165.9, 165.7, 137.3–139.9 (154.5 for **8a/9a**), aromatic and  $\text{CH}(\text{CF}_3)_2$  signals, and a singlet at 59.1–59.7,  $\Delta\text{C}_{\alpha,\beta} > 105$  ppm.

**Chemical Shifts of HCl in DMF- $d_7$  and DMSO- $d_6$ .** When a small amount of gaseous HCl was bubbled into pure DMF- $d_7$  at rt, a broad signal appeared at  $\delta$  8.88, and the DMF signals  $\delta$  2.74, 2.91, and 8.01 at rt shifted upfield by 0.05 ppm. With higher HCl concentration (7% of the DMF concentration) the signal became a sharp signal at  $\delta$  14.12, and the DMF signals shifts were negligible. At 220 K the signal became broad at ca.  $\delta$  15.25. When the rt spectrum was measured after 72 h, the lower field signal shifted to  $\delta$  13.79, other signals were not affected, and a new broad signal at  $\delta$  9.74 (intensity 3% of  $\delta$  13.79 signal), which may be due to decomposition to HCOOH, is obtained. We conclude that  $\delta(\text{H}^+)$  in DMF  $\geq 8.88$ , depending on the temperature and concentration.

In DMSO- $d_6$  containing traces of water, small amount of bubbled HCl did not cause any change, but when the  $[\text{HCl}]$  was ca. 20% of that of  $[\text{DMSO-}d_6]$ , the water signal disappeared, a sharp signal appeared at  $\delta$  13.30, and the DMSO signal was not affected.

**Z-Enol/E-Enol Chemical Shifts and Ratios.** Only one enol is observed for **7a–d** in  $\text{CDCl}_3$ , but two enols were observed for **9a–d** at 240 K. In THF- $d_8$  and in  $\text{CD}_3\text{-CN}$ , two enols were observed in the  $^1\text{H}$  NMR for all the systems but the OH signal of **E-7a–7d** was not observed

(7) Lei, Y. X.; Rappoport, Z. *J. Org. Chem.* **2002**, *67*, 6971.



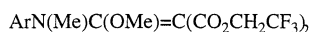
**TABLE 9.** DNMR Data Related to Rotation around the C=C Bond in THF-*d*<sub>8</sub>

comp	$K_{i,c}^a$	$T_c$ , K	$k_c, ^b s^{-1}$	$\Delta G_c^\ddagger, ^c kcal/mol$
<b>7a</b>	7	302	56	15.3, 16.5
<b>7d</b>	5	> 330 <sup>d</sup>	> 54	> 16.9, > 17.9
<b>9b</b>	8.2	270.8	54.2	13.7, 14.8
<b>9d</b>	1.5	284.6	65.1	14.5, 14.8
<b>3a</b>				18.7 <sup>e</sup>
<b>12a</b>				9.4 <sup>f</sup>
<b>12b</b>				10.0 <sup>f</sup>

<sup>a</sup>  $K_{i,c}$  is the equilibrium ratio of the two enols at the coalescence temperature, calculated from a  $\log K_i$  vs  $1/T$  plot. <sup>b</sup> At the coalescence temperature  $T_c$ . <sup>c</sup> The two  $\Delta G_c^\ddagger$  values are for the processes starting from the *Z*-isomer and the *E*-isomer, respectively. Estimated errors are  $\pm 0.3$  kcal/mol. <sup>d</sup> Coalescence starts but is incomplete at 330 K, close to the bp of THF. <sup>e</sup> In C<sub>6</sub>D<sub>6</sub>, from ref 3. <sup>f</sup> From ref 7.

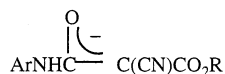
in both solvents and for **E-9a** in CD<sub>3</sub>CN at 240–298 K. The OH signal is observed in THF-*d*<sub>8</sub> for **9a–9d** at 200–240 K and for **7a–7d** at 220 K. The following features are discernible from Table 3: (i) always  $\delta(OH, \mathbf{7a-7d}) > \delta(OH, \mathbf{9a-9d})$ , (ii) always  $\delta(NH, \mathbf{9a-9d}) > \delta(NH, \mathbf{7a-7d})$ , (iii) the  $\delta(NH)$  values are solvent dependent, and for both series their order is CDCl<sub>3</sub> < CD<sub>3</sub>CN < THF-*d*<sub>8</sub>, (iv) when both enols were observed, the  $\Delta\delta(OH) = \delta(OH, Z\text{-enol}) - \delta(OH, E\text{-enol})$  is higher for system **7** than for system **9**, (v) the  $\Delta\delta(NH) = \delta(NH, Z\text{-enol}) - \delta(NH, E\text{-enol})$  is higher for **7** than for **9** in THF-*d*<sub>8</sub>, (vi) for **9**, the order of  $\Delta\delta(NH)$  is CDCl<sub>3</sub> > CD<sub>3</sub>CN > THF-*d*<sub>8</sub>.

**DNMR Study.** The presence of two enols at low temperature and of one enol with a broad OH signal in a few cases at rt suggest that a coalescence process takes place around or below rt. The behavior of the CH signal was studied for **9b** and **9d** by DNMR. The coalescence temperatures  $T_c$  in THF-*d*<sub>8</sub> were 270.8 and 284.6 K, respectively. By using the populations of the two isomers at  $T_c$ , the  $\Delta G_c^\ddagger$ s values were found to be 13.7 and 14.5 kcal/mol, respectively, starting from the *Z*-enols, and 14.8 kcal/mol starting from both *E*-enols. These values are between the values for the *O,N*-dimethyl systems **12a**



**12** (a) Ar = *p*-MeOC<sub>6</sub>H<sub>4</sub>

(b) Ar = *p*-MeC<sub>6</sub>H<sub>4</sub>



**13 a-d:** R = CH<sub>2</sub>CF<sub>3</sub> (a-d are as in systems 6/7)

**14 a-d:** R = CH(CF<sub>3</sub>)<sub>2</sub>

and **12b** and that for **3a** (Table 9).

The DNMR study of compounds **7** is complicated by the presence of both enols and amides, but a coalescence study of the CH<sub>2</sub> quartet was possible. Compound **7a** showed coalescence at 302 K and  $\Delta G_c^\ddagger$  of 15.3 and 16.5 kcal/mol starting with the *Z*- and *E*-enol, respectively. A sample of **7d** in THF-*d*<sub>8</sub> showed broadening, but no coalescence up to 330 K, giving a minimum  $\Delta G_c^\ddagger$  value of 16.9 kcal/mol starting from **Z-7d**.

**Temperature Dependence of the Enol/Amide and the Z-Enol/E-Enol Equilibria.** In the range 180–298 K the <sup>1</sup>H, <sup>19</sup>F, and <sup>13</sup>C NMR spectra display separate signals with no coalescence for the amide and the enol(s) for all systems in all solvents. However, the percentage

**TABLE 10.** Thermodynamic Parameters for the Enol ⇌ Amide and Z-enol ⇌ E-enol Equilibria in THF-*d*<sub>8</sub> at 298 K

system	$K_{\text{Enol}}$ or $K_i$	$\Delta G^\circ$ kcal/mol	$\Delta H^\circ$ , kcal/mol	$\Delta S^\circ$ , eu
<b>6a ⇌ 7a</b>	10 <sup>a</sup>	-1.4	-1.2	0.8
<b>6c ⇌ 7c</b>	5.4 <sup>a</sup>	-1.0	-0.5	1.7
<b>6d ⇌ 7d</b>	4.3 <sup>a</sup>	-0.9	-0.5	1.1
<b>8d ⇌ 9d</b>	9.0 <sup>a</sup>	-1.3	-2.3	-3.3
<b>Z-7a ⇌ E-7a</b>	6.7 <sup>b</sup>	-1.1	-1.1	0.1
<b>Z-7c ⇌ E-7c</b>	6.0 <sup>b</sup>	-1.1	-0.3	2.6
<b>Z-7d ⇌ E-7d</b>	4.5 <sup>b</sup>	-0.9	-0.5	0.2
<b>Z-9a ⇌ E-9a</b>	1.7 <sup>b</sup>	-0.4	-1.0	-2.2
<b>Z-9b ⇌ E-9b</b>	1.6 <sup>b</sup>	-0.3	-0.9	-2.1
<b>Z-9d ⇌ E-9d</b>	1.5 <sup>b</sup>	-0.2	-1.4	-3.9

<sup>a</sup>  $K_{\text{Enol}}$ . <sup>b</sup>  $K_i$ .

of the amide in THF-*d*<sub>8</sub> increased upon an increase in the temperature (Table 7).  $\log K_{\text{Enol}}$  vs  $1/T$  plots were linear and gave the  $\Delta H^\circ$  values. The  $\Delta G^\circ$  and  $\Delta S^\circ$  were calculated from them and the  $K_{\text{Enol}}$  value at 298 K. The data are in Table 10.

The *Z*-enol/*E*-enol ratios in THF-*d*<sub>8</sub> were determined at 180–280 K. The percent of *E*-enol increased upon a decrease in temperature. Plots of  $\log([Z\text{-enol}]/[E\text{-enol}])$  vs  $1/T$  were linear ( $R^2 > 0.99$ ), giving the thermodynamic parameters in Table 10.

## Discussion

**Cyano vs Ester Effects.** Although information on stable enols of amides is slowly accumulating, the only systematic data on the structures and  $K_{\text{Enol}}$  values as a function of the structure and the solvent are for the diester activated systems **3**.<sup>3</sup> In enol/amide systems **3/4** one ester group (CO<sub>2</sub>CH<sub>2</sub>CF<sub>3</sub> or CO<sub>2</sub>CH(CF<sub>3</sub>)<sub>2</sub>) is identical with that in the presently studied systems **6/7** and **8/9**, and we can evaluate the effect of replacing one such ester group by a cyano group. A more limited comparison is that of **7a** and **9a** with the CN, CO<sub>2</sub>Me activated system **10**.

Cyano is a better inductively EW group than CO<sub>2</sub>Et ( $\sigma_I$ , CN, 0.55; CO<sub>2</sub>Et, 0.30),<sup>8</sup> but resonatively the two groups are similar ( $\sigma_R$ , CN, 0.13; CO<sub>2</sub>R, 0.14;  $\sigma_R^-$ , CN, 0.33; CO<sub>2</sub>R, 0.34).<sup>8</sup> Cyano has a lower steric bulk than an ester, and due to its linearity, it better accommodates into a planar resonative system. Consequently, cyano is a better acidifying group than a CO<sub>2</sub>Me or even a CO<sub>2</sub>-CH<sub>2</sub>CF<sub>3</sub> group, of polysubstituted carbon acids ( $pK_a$ - (DMSO)/CH<sub>2</sub>(CN)X/ 14.2 (X = CO<sub>2</sub>Et), 11.2 (X = CN), and  $pK_a = 16.4$  for CH<sub>2</sub>(CO<sub>2</sub>Me).<sup>9</sup> Relevant data to our systems are the ICR determined  $\Delta H_{\text{ionization}}(\text{CH}_2\text{YY}')$  [gas phase, kcal/mol] values. PhNHCOCHYY': YY = (CO<sub>2</sub>-Me)<sub>2</sub>, 324.1; CO<sub>2</sub>CH<sub>2</sub>CF<sub>3</sub>(CO<sub>2</sub>Me), 317.9; (CO<sub>2</sub>CH<sub>2</sub>CF<sub>3</sub>)<sub>2</sub>, 311.4; CO<sub>2</sub>Me(CN), 309; CN(CO<sub>2</sub>CH<sub>2</sub>CF<sub>3</sub>), 304.0; CO<sub>2</sub>CH<sub>2</sub>-(CF<sub>3</sub>)<sub>2</sub>(CN), 302.7.<sup>10</sup> These differences should also be

(8) Lowry, T. H.; Richardson, K. S. In *Mechanism and Theory in Organic Chemistry*, 3rd ed.; Harper and Row: New York, 1987; pp 154–157.

(9) Bordwell, F. G. *Acc. Chem. Res.* **1988**, *21*, 456.

(10) (a) Mishima, M.; Lei, Y. X.; Rappoport, Z. 16th IUPAC Conference on Physical Organic Chemistry (ICPOC 16), University of California, San Diego, La Jolla, California, 4–9 August, 2002, Book of Abstracts, Abst. LC21 and unpublished results. (b) Solvent effects should affect the values in solution. However, we note that SCRF calculations indicate only a small solvent effect of CCl<sub>4</sub> or EtOH on the gas-phase  $K_{\text{Enol}}$  values.<sup>4a</sup> Moreover, the hydrogen bonds which affect strongly the  $K_{\text{Enol}}$  values are not treated in these calculations.

reflected in the stabilization of the zwitterionic hybrid **1a** of the enol. In addition, the dipole moments of CN and COOR and the interaction of their dipoles with the CO of **2** and the C–O of **1** differ. Moreover, the ester carbonyl is a better hydrogen bond acceptor from the OH and NHR groups than a CN group.

Several of these properties operate in opposite directions on the relative stabilization of **1** and **2**, and predictions of whether the  $K_{\text{Enol}}$  values for systems **6/7** and **8/9** are higher than, identical to, or lower than those for systems **3/4** are difficult to make.

A previous experiment with the CN, CO<sub>2</sub>Me activated system **5/10**, showed it to be the enol **10** in the solid state with intramolecular COOR...HO and intermolecular NH...CN hydrogen bonds. Since the (CO<sub>2</sub>Me)<sub>2</sub> analogue **3a/4a** (Ar = Ph) and the diesters **3b/4b** (various Ar) have the amide structures **4a** and **4b** in the solid state,<sup>2,3</sup> a cyano is a better enol stabilizer than CO<sub>2</sub>Me or CO<sub>2</sub>CH<sub>2</sub>CF<sub>3</sub> in the solid. This is also true in solution. In CDCl<sub>3</sub> at rt, the **3a/4a**,<sup>2</sup> **3b/4b**, **3c/4c**, and **3d/4d**<sup>3</sup> mixtures are 5%, 26%, 78–83%, and 81–88% enolic,<sup>3</sup> respectively, whereas at 220 K, **10** is the only species, and at 298 K all systems **6/7** and **8/9** are exclusively enolic. In THF-*d*<sub>8</sub>  $K_{\text{Enol}} = 0.4$  for **3a/4a** and 10 for **7a**, i.e.;  $K_{\text{Enol}}$  increases 25-fold by replacing a CO<sub>2</sub>CH<sub>2</sub>CF<sub>3</sub> group by a CN. In CD<sub>3</sub>CN  $K_{\text{Enol}} = 1.0$ – $2.3$  for **7a–d** and  $3.5$ – $9.0$  for **9a–d** at 298 K,  $K_{\text{Enol}}(\mathbf{9})/K_{\text{Enol}}(\mathbf{7}) = 3.2$ – $3.9$ . For **3d/4d**  $K_{\text{Enol}} = 0.03$ – $0.08$ . For **3e/4e** the  $K_{\text{Enol}} = 0.23$  (Ar = Ph) and  $0.33$  (Ar = *p*-MeC<sub>6</sub>H<sub>4</sub>) while  $K_{\text{Enol}} = 5.7$  (**9b**) and  $5.3$  (**9c**). Consequently, the CN increases  $K_{\text{Enol}}$  by 17–140-fold, compared with CO<sub>2</sub>CH<sub>2</sub>CF<sub>3</sub> and by only 6-fold compared with CO<sub>2</sub>CH(CF<sub>3</sub>)<sub>2</sub>, and appreciable percentages of the CN-substituted enols are observed in THF-*d*<sub>8</sub> and CD<sub>3</sub>CN, whereas the di-CO<sub>2</sub>R-enols are a very minor component in CD<sub>3</sub>CN.<sup>3</sup>

**Ionization of the Enols/Amides in DMSO-*d*<sub>6</sub> and DMF-*d*<sub>7</sub>.** Only the amide was previously observed in DMSO-*d*<sub>6</sub> for all systems, including **3/4**.<sup>2,3</sup> The higher stability of enols **7**, **9** and the higher acidity of **6/7**, **8/9** can open two new possibilities. The enols may be observable in DMSO-*d*<sub>6</sub>, or ionization of the **6/7**, **8/9** systems will give the resonative enolate ions in the polar solvent. Since DMF-*d*<sub>7</sub> resembles DMSO-*d*<sub>6</sub> in its polarity, solvent properties, and behavior but could be cooled to a low temperature, in contrast with DMSO-*d*<sub>6</sub>, most of the experiments were conducted in DMF-*d*<sub>7</sub>. The conclusions are similar for both solvents.

<sup>1</sup>H, <sup>19</sup>F, and <sup>13</sup>C NMR spectra in both solvents show the presence of one major species together with at most a few percent of another species. The major species is neither an enol, since its low field signal is not in the relatively narrow region of  $\delta(\text{enolic OH})$  and it is a much broader signal, nor an amide, since it lacks a C <sub>$\beta$</sub> H signal at the CH region of amides **4** and **5**. The minor product has such a C <sub>$\beta$</sub> H signal and is probably the amide.

A change to highly polar solvents is expected to enhance the ionization of the amide/enol species, which is substituted by three strongly EW substituents. In the similar situation of the diesters **3/4**, the derived anions carry three bulky substituents and planarity, and hence, maximum stabilization by resonative negative charge delocalization on Y, Y' is not achieved. In the cyano-substituted anions **13** and **14** derived from **6/7** or **8/9**, planarity is more easily achieved due to the linear CN

group, delocalization is more efficient, and, hence, the ionization should be more extensive than in the non-CN activated systems. Indeed, the gas phase  $\Delta H_{\text{ionization}}$  values quoted above for **7a** and **8a/9a** are ~20 and 21 kcal/mol more favored than those for **3a/4a** and ~7 and 8 kcal/mol more favored than those for **3d/4d**.<sup>10</sup> Hence, ionization of **6/7**, **8/9** is the dominant process in the polar solvents.

There are precedents. The acidic polymethoxycarbonylcyclopentadienes<sup>11</sup> and compounds (NC)<sub>2</sub>CHCO<sub>2</sub>R<sup>12</sup> ionize in DMSO-*d*<sub>6</sub>, although they have the enol of ester structure in less polar solvents such as CDCl<sub>3</sub>.

That addition of NaOH to the solution in DMF-*d*<sub>7</sub> and DMSO-*d*<sub>6</sub> does not affect the spectra, except for the disappearance of the very broad lower field proton (see below) and the minor species (which we ascribe to **6** or **8**, which ionizes by the added base) corroborates that the observed spectra are for the already ionized species, i.e., anions **13a–d** and **14a–d**. Likewise, in the less polar THF where the enols and the amide are observed, the addition of base give species that we ascribe to the anions **14b,c** (Table 6). The observed spectra raise two questions: (i) Is the broad low field signal due to the solvated proton (H<sup>+</sup>·S, S = DMF, DMSO)? (ii) Are the chemical shifts of the observed species consistent with expectation for ions **13** and **14**?

The spectra of HCl in DMSO-*d*<sub>6</sub> and DMF-*d*<sub>7</sub> answer question (i) in the affirmative. The broad signal observed at low HCl concentration resembles, in its broad shape and its  $\delta$  value, the signal of our systems observed in DMF-*d*<sub>7</sub> in several cases. The formation of a sharper signal at rt and a broader one at low temperature at higher HCl concentration indicate that association and hydrogen bonds strongly effect the position and shape of the H<sup>+</sup>·S signal. A rapid exchange of H<sup>+</sup>·S with the solvent S probably makes the  $\delta$  value concentration dependent.

A simplified expectation is that <sup>1</sup>H, <sup>13</sup>C, and <sup>19</sup>F signals of **13** and **14** will shift upfield compared with the neutral precursors as is known for carbanions derived from carbon acids.<sup>13a</sup> However, for systems carrying the strongly EW CN and CO<sub>2</sub>R substituents, we cannot predict the direction of the shift as shown by the following examples: For CH<sub>2</sub>(CO<sub>2</sub>Me)<sub>2</sub>  $\delta$  41.2 (CH<sub>2</sub>), 167.6 (CO<sub>2</sub>Me), 52.3 (Me),<sup>13b</sup> and in its carbanion Na<sup>+</sup>C<sup>-</sup>H(CO<sub>2</sub>Me)<sub>2</sub>  $\delta$ -(HMPT) = 61.3, 171.9, and 47.8, <sup>13c</sup> i.e., both the formal carbanionic carbon and the CO<sub>2</sub> carbon are shifted to a low field. In contrast, for CH<sub>2</sub>(CN)<sub>2</sub>,  $\delta$  8.6 (CH<sub>2</sub>) and 110.5 (CN)<sup>13d</sup> are shifted to -2.1 and 130.3, i.e., upfield for the C<sup>-</sup> and low field for the CN in Na<sup>+</sup>CH(CN)<sub>2</sub> in HMPT.<sup>13c</sup>

In our systems, the ground-state polarization is very high, judging by the  $\Delta\delta_{\alpha,\beta}$  of >100 ppm. The  $\delta(\text{COOR})$  values of 170.2–172.7 for enols **Z-7a–d** and **Z-9a–d** in CD<sub>3</sub>CN, CDCl<sub>3</sub>, and THF-*d*<sub>8</sub> are in the region of the C<sup>-</sup>H(CO<sub>2</sub>Me)<sub>2</sub> anion. Ionization of such systems should not change drastically the charge on C <sub>$\alpha$</sub> , C <sub>$\beta$</sub> , and their substituents. The  $\delta(\text{COOR})$  of 165.6–169.13 in **13** and

(11) Lei, Y. X.; Cerioni, G.; Rappoport, Z. *J. Org. Chem.* **2000**, *65*, 4028.

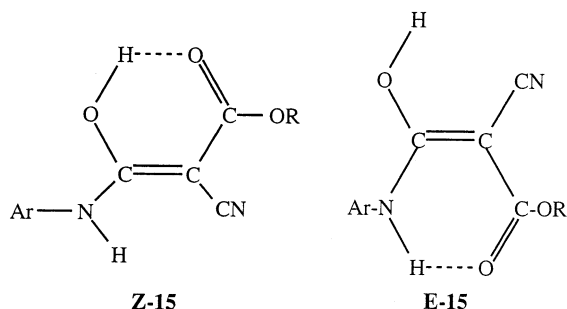
(12) Neidlein, R.; Kikelj, D.; Kramer, K.; Sui, Z.; Boese, R.; Blaser, D.; Kocjan, D. *Chem. Ber.* **1989**, *122*, 1341.

(13) Kalinowski, H.-O.; Berger, S.; Brown, S. In *Carbon-13 NMR Spectroscopy*; Wiley: Chichester, U.K., 1984; (a) p 415, (b) p 206, (c) p 418, (d) p 249.

**14** are not unreasonable, and the shifts of  $C_\beta$  from  $\delta$  57.4–58.9 in THF- $d_8$  mostly to 59.1–60.7 are in the direction found in the malonic ester system. Moreover, these shifts resemble those observed on ionization in THF where the anions **14c** (Table 6) and **14b** are presumably formed. We conclude that the small changes observed in  $\delta$   $^{13}\text{C}$  values are as expected due to the high polarization in the enols and that the direction of the shifts is not inconsistent with an ionization process.

**Hydrogen Bonding in the Enols.** The importance of hydrogen bonding between the OH, and to a lesser extent the NH group and cis ester groups, was emphasized in our work on systems **3**.<sup>3</sup> It was concluded that the  $\text{OH}\cdots\text{O}=\text{COR}$ -cis interaction is the dominant one, it occurs preferentially with the less fluorinated ester group, and contributes to the barrier for internal rotation around the  $\text{C}=\text{C}$  bond in the push-pull enols.<sup>3,7</sup> The stronger hydrogen bond in the *Z*-isomer leads to a higher  $\delta$  (OH) value and to its preference in the *E/Z* enol equilibria.

In enols **7** and **9**, there is only one ester group which enables an OHO intramolecular hydrogen bond in the *Z*-isomer, **Z-15**. The CN group is too remote to allow intramolecular  $\text{OH}\cdots\text{NC}$  and  $\text{NH}\cdots\text{NC}$  bonding in solution, although in the solid, the *Z*-isomer forms such an intermolecular hydrogen bond. By the concentration-independent shifts, we exclude such strong interaction in solution. However, a weaker NHO hydrogen bond exists in the *E*-isomer, **E-15**.



The prediction is that **Z-15** will be the major or the exclusive isomer. However, in **7** and **9**, where the ester group carries three or six fluorines, the hydrogen bonds are weaker in **9** than in **7**, and in **7** and **9** than in **Z-3d,e** and **10**. Due to the hydrogen bonds, we expect in non-hydrogen bonding solvents a lower field  $\delta$ (OH) for **Z-15**,<sup>14</sup> a lower field NH for **E-15**, a lower internal rotation barrier than in the diesters **3**, higher **Z-7/E-7** than **Z-9/E-9** ratios, and a modification of these predictions in hydrogen bonding solvents.

The single enol observed for **7a-d** in  $\text{CDCl}_3$  and  $\text{CD}_3\text{CN}$  where data only at 298 K are available is unlikely to be due to the exclusive formation of **Z-7**, since in THF- $d_8$ , the NH signals of both enols are observed at 298 K. Hence, we ascribe it to a rapid **Z-7**  $\rightleftharpoons$  **E-7** interconversion at 298 K as measured in other systems.<sup>15</sup> The OH signal of **E-7** is not observed due to its low intensity and to broadening due to hydrogen bonding to the solvent. As

expected, the OH signals of **E-7** and **E-9** are observed only at low temperature (220 K for **7a**, 200 and 240 K for **9a-9d** in THF- $d_8$ ).

The few  $\delta$ (OH) values available for **E-15** are at a significantly higher field than for **Z-15**. The  $\delta$ (OH) values are also at a higher field than for the diesters **3**, since in both **E-** and **Z-3** there are  $\text{OH}\cdots\text{O}=\text{COR}$  bonds. Both observations are according to the predictions.

A stronger hydrogen bond to the  $\text{CO}_2\text{CH}_2\text{CF}_3$  in **7** than for the  $\text{CO}_2\text{CH}(\text{CF}_3)_2$  for **9** is reflected by several phenomena. First,  $\delta$ (OH) for **7** is 0.7–1.0 ppm higher than that for **9** in  $\text{CDCl}_3$ ,  $\text{CD}_3\text{CN}$ , and in THF- $d_8$  at 240 K. Second,  $\delta$ (OH) [**Z-7-E-7**] >  $\delta$ (OH) [**Z-9-E-9**]. Third,  $\delta$ (NH) (**7**) <  $\delta$ (NH) (**9**) but the differences (0.2 in  $\text{CD}_3\text{CN}$ , 0.4 in  $\text{CDCl}_3$ , 0.3–0.6 in THF- $d_8$ ) are not large. Fourth, the *Z*-enol/*E*-enol ratios are relatively high in  $\text{CD}_3\text{CN}$  for all systems and for **7a-7d** in THF- $d_8$ , where the *Z*-isomers comprise 90% and 70–81% of the enols mixture systems.

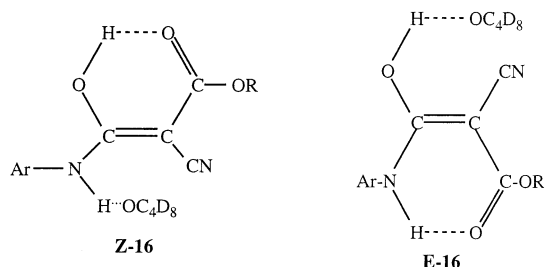
The significant temperature dependence of the **E-9/Z-9** in THF- $d_8$  leads to 62% **Z-9** in the enol mixture at 280 K but to only 27–38% at 180 K; i.e., the stabilities of both enols in THF- $d_8$  are approximately similar. The intermolecular OHO hydrogen bond to the solvent of the *E*-isomer competes with the intramolecular bond in the *Z*-enol. Nevertheless, when both OH signals are observed, those of **Z-9** are at a significantly lower field than that for **E-9**.

Only one OH signal appears at rt for compounds **9** at  $\delta$  11.50–11.89, i.e., at a significantly higher field than for the enol in other solvents or at lower temperatures (e.g., for **Z-9** at lower temperatures  $\delta$ (OH) = 13.24–13.50). The temperature-dependent spectra of **9a**, **9b**, and **9d** indicate an interconversion process of the two enols. Significantly, the two OH signals have a different shape: the lower field signal for **Z-9** is sharp, whereas the upper field signal for **E-9** is broad. Moreover, upon an increase in temperature, both signals broaden, but the signal for **Z-9** shows a minor shift, whereas that for **E-9** shifts significantly to an upper field (e.g., for **9d** from  $\delta$  11.17 (180 K) to 8.87 (220 K)). The NH signals behave similarly, but to a much lower extent. The lower field signal for **E-9** does not shift significantly, while that for **Z-9** shifts systematically, e.g., for **Z-9d** from  $\delta$  10.56 (180 K) to 10.11 (280 K), with gradual broadening until they coalesce at ca. 300 K. These shifts complicate a DNMR study by using the NH signals, but the two  $\text{HC}(\text{CF}_3)_2$  heptets of the two enols shift almost to the same extent (from  $\delta$  6.86, 7.00 (180 K) to 6.50, 6.65 (260 K), enabling such a study.

A consistent picture emerges from these data. THF- $d_8$  is a better hydrogen bond acceptor than  $\text{CDCl}_3$  and probably  $\text{CD}_3\text{CN}$ . Whereas in systems **3**, where both the OH and the NH groups are intramolecularly hydrogen bonded to cis-ester groups, in systems **7** and **9**, only one such ester group is present, and only one intramolecular bond is present in **Z-15** and **E-15**. In THF in **Z-16**, the OH is hydrogen bonded to the  $\text{CO}_2\text{R}$  group, forming a stronger bond than the  $\text{NH}\cdots\text{O}=\text{COR}$  hydrogen bond in **E-16**. The NH group of **Z-16** or the OH group of **E-16** intermolecularly hydrogen bond to the oxygen of the solvent ( $\text{OC}_4\text{D}_8$ ), and such interaction is typically weakened upon an increase in temperature. Since the stronger hydrogen bonds cause a shift of  $\delta$ (OH) and  $\delta$ (NH) to a

(14) Perrin, C. L.; Nelson, J. B. *Annu. Rev. Phys. Chem.* **1997**, *48*, 511.

(15) E.g.; Sandström, J. In *The Chemistry of Enamines*; Rappoport, Z., Ed.; Wiley: Chichester, U.K., 1994; Chapter 6.



lower field, upon temperature increase, the OH of **E-16** and the NH of **Z-16** shift to a higher field, and the effect is larger for the stronger intermolecular O–H···O bond of **E-16**. The intramolecular OH···O=C bond in **Z-16** or the NH···O=C bond in **E-16** is almost temperature independent, and  $\delta(\text{OH})$  and  $\delta(\text{NH})$  shift only slightly (Table 4).

The reduced hydrogen bond to the solvent at the higher temperature therefore affects more the OH···O bond in **E-16** than the already weaker NH bond in **Z-16**, and the relative stability of **Z-16** increases. Consequently, the *Z*-enol/*E*-enol ratio increases with the temperature (Table 7).

The intramolecular hydrogen bond to the  $\text{CO}_2\text{CH}(\text{CF}_3)_2$  group of enols **9** is weaker than that to the  $\text{CO}_2\text{CH}_2\text{CF}_3$  group of **7** or of **3**. Consequently, the hydrogen bond stabilization of **9** with THF is of the same magnitude as the intramolecular stabilization at low temperature, making **E-16** similarly or more stable at the low temperature.

The intramolecular OHO hydrogen bond is a configuration holder for **Z-16**, but with the increase of the temperature an enhanced competition from internal rotation around the C=C bond in the push–pull **Z-16** leads to a rapid *Z* ⇌ *E* interconversion, to an observed coalescence below rt, and to a single averaged OH signal at a  $\delta(\text{OH})$  value between those for **Z-16** and **E-16**. Many rotational barriers in push–pull alkenes were measured by DNMR, and the values in Table 9 resemble values measured for related systems.<sup>15</sup> In our systems, the barriers have a significant contribution from the intramolecular hydrogen bond. Hence,  $\Delta G_c^\ddagger$  for the internal rotation around the C=C bond in **7** and **9** is higher than that for compounds **12**, which are incapable of forming such bonds, but lower than for **3a**, having two intramolecular hydrogen bonds to the  $\text{CO}_2\text{CH}_2\text{CF}_3$  group which are stronger than that for the  $\text{CO}_2\text{CH}(\text{CF}_3)_2$  bond in **Z-16**. This is consistent with the behavior of system **7**, whose OH···O=C bond resembles that in **3**. The difference between the barriers for **7** and **9** and those for **12a,b** give minimum values for the strengths of the intramolecular hydrogen bonds.

The higher stabilities of enols **Z-7** than those of **Z-9** lead to higher *Z-7/E-7* than the *Z-9/E-9* ratios. Moreover, at rt, the  $\delta(\text{OH})$  observed for the “single enol” resembles that of **Z-7**, indicating that the latter is the major constituent in the rapidly equilibrating *Z-7/E-7* mixture. The rotational barrier for **7a** is higher than in **9b,c**.

For enol **10** (the  $\text{CO}_2\text{Me}$  analogue of **7c** and **9c**) in  $\text{CDCl}_3$ , the only one OH signal at 243 and 220 K indicates that only **Z-10** is observable, whereas both **E-7** and **E-9** were observed at low temperatures. This is consistent with the stronger O–H···O=C–OR hydrogen bond when R = Me than when R =  $\text{CH}_2\text{CF}_3$  or  $\text{CH}(\text{CF}_3)_2$  of **7a** and

**9a**. The stronger hydrogen bond in **Z-10** is also reflected in its  $\delta(\text{OH})$  at 15.15 (220 K) and ca. 15.4 (rt) and in the  $\delta(\text{NH})$  of 8.95 (220 K) in  $\text{CDCl}_3$ . The  $\delta(\text{OH})$  value is ca. 1 and 1.8 ppm higher and the  $\delta(\text{NH})$  value is ca. 0.9 and 0.7–0.6 higher than those for **7a–d** and **9a–d**, respectively. Since the NH of **7a**, **9a**, and **Z-10** is not intramolecularly bonded, the difference in  $\delta(\text{NH})$  reflects the effect of the R in the hydrogen bonded OH···O=COR moiety on  $\delta(\text{NH})$ . However, since  $\delta(\text{OH})$  and  $\delta(\text{NH})$  values of **7a** and **9a** in  $\text{CDCl}_3$  are average values of the *E*- and *Z*-enols, this conclusion is not unequivocal.

In THF-*d*<sub>8</sub> both enols of **10** are observed, and  $\delta(\text{OH})$  and  $\delta(\text{NH})$  for **Z-10** at 220 K are 15.5 and 9.94 ppm, respectively, whereas  $\delta(\text{NH})$  for **E-10** is 11.27. The  $\delta(\text{OH})$  of **10** is 1.2 and 2.0 ppm to a lower field than in the *Z* isomers of **7** and **9**, and  $\delta(\text{NH})$  is 0.1 and 0.5 ppm to an upper field. For **E-10**, the corresponding  $\delta(\text{NH})$  values are 0.5–0.6 ppm to a lower field (Table 3). Unequivocally, the OH···O=C–OR bond is stronger for R = Me than for R =  $\text{CH}_2\text{CF}_3$  or  $\text{CH}(\text{CF}_3)_2$ .

Comparison with the published  $\delta(\text{OH})$  and  $\delta(\text{NH})$  values for **3d** and **3e**<sup>3</sup> suffers from the fact that the values in  $\text{CDCl}_3$  for **7** and **9** are averages, while in  $\text{CD}_3\text{CN}$  enols **3** were barely observed.<sup>3</sup> Nevertheless, it is clear even from the average values and by comparing the  $\delta(\text{OH})$  and  $\delta(\text{NH})$  values for **Z-10** in  $\text{CDCl}_3$  with those of 17.06, 11.2–11.5 for **3b,c** Ar = Ph, that both values are at a lower field for **3** than for **10**. Here, the effect of CN is compared with that of a  $\text{CO}_2\text{R}$  not hydrogen bonded to the OH. The more EW cyano weakens the OH···O=C bond more than  $\text{CO}_2\text{R}$ , and thus reduces, more than  $\text{CO}_2\text{R}$ , the electron-density of the H-bond donor oxygen of the C=O. This is in line with the conclusion drawn above.

The effect of  $\text{CO}_2\text{CH}_2\text{CF}_3$  vs CN on the hydrogen bonding in a HO···OCOCH<sub>2</sub>CF<sub>3</sub> moiety is obtained by comparing the  $\delta(\text{OH})$  and  $\delta(\text{NH})$  of 16.02 and 10.54 for **3d**, Ar = *p*-MeOC<sub>6</sub>H<sub>4</sub><sup>3</sup> with 14.00 and 9.61, respectively, for **7a** in THF-*d*<sub>8</sub> at 298 K. Since the latter values differ by 0.3–0.4 ppm from those for **Z-7** at 298 K, a  $\text{CO}_2\text{CH}_2\text{CF}_3$  causes at least 1.5 ppm downfield shift of a hydrogen-bonded  $\text{CO}_2\text{CH}_2\text{CF}_3$  to OH and 1.5 ppm upfield shift for an NH than CN. Again, this is in line with our generalizations.

## Experimental Section

**General Methods.** Melting points, <sup>1</sup>H, <sup>13</sup>C, and <sup>19</sup>F NMR spectra were measured as described previously.<sup>16</sup> Solid-state <sup>13</sup>C NMR spectra were measured as described in ref 3.

**Solvents and Materials.**  $\text{CDCl}_3$ , THF-*d*<sub>8</sub>, DMSO-*d*<sub>6</sub>, DMF-*d*<sub>7</sub>, and the starting materials (commercially obtained) were used without further purification.

**Crystallographic Data. 9b:** C<sub>14</sub>H<sub>10</sub>F<sub>6</sub>N<sub>2</sub>O<sub>3</sub>. Space group P $\bar{1}$ : *a* = 11.631(4) Å, *b* = 15.036(5) Å, *c* = 10.028(3) Å,  $\alpha$  = 93.55(3)°,  $\beta$  = 108.67(3)°,  $\gamma$  = 70.51(3)°, *V* = 1564(1) Å<sup>3</sup>, *Z* = 4,  $\rho_{\text{calcd}}$  = 1.56 g cm<sup>-3</sup>,  $\mu(\text{Cu K}\alpha)$  = 14.11 cm<sup>-1</sup>; no. of unique reflections, 5736; no. of reflections with *I* ≥ 3 $\sigma$ <sub>*I*</sub>, 3450; *R* = 0.060, *R*<sub>w</sub> = 0.086; **7a:** C<sub>13</sub>H<sub>11</sub>F<sub>3</sub>N<sub>2</sub>O<sub>4</sub>. Space group P1: *a* = 10.244(6) Å, *b* = 13.334(6) Å, *c* = 5.37(1) Å,  $\alpha$  = 96.4(1)°,  $\beta$  = 98.9(1)°,  $\gamma$  = 73.87(4)°, *V* = 694(1) Å<sup>3</sup>, *Z* = 2,  $\rho_{\text{calcd}}$  = 1.51 g cm<sup>-3</sup>,  $\mu(\text{Cu K}\alpha)$  = 12.21 cm<sup>-1</sup>; no. of unique reflections, 2537; no. of reflections with *I* ≥ 2 $\sigma$ <sub>*I*</sub>, 1908; *R* = 0.093, *R*<sub>w</sub> = 0.129.

**Trifluoroethyl Cyanoacetate.** To a mixture of 2,2,2-trifluoroethanol (20 g, 0.2 mol) and dimethylaniline (24.2 g,

(16) Frey, J.; Rappoport, Z. *J. Org. Chem.* **1997**, *62*, 8327.

TABLE 11. Analytical Data and Yields for *p*-XC<sub>6</sub>H<sub>4</sub>NHC(OH)=C(CN)CO<sub>2</sub>R<sup>a</sup>

compound		formula	mp, °C	yield, %	calculated, %			found, %		
X	R				C	H	N	C	H	N
MeO	CH <sub>2</sub> CF <sub>3</sub>	C <sub>13</sub> H <sub>11</sub> F <sub>3</sub> N <sub>2</sub> O <sub>4</sub>	290–2	94	49.38	3.50	8.86	49.06	3.75	8.65
Me	CH <sub>2</sub> CF <sub>3</sub>	C <sub>13</sub> H <sub>11</sub> F <sub>3</sub> N <sub>2</sub> O <sub>3</sub>	>300	96	52.01	3.69	9.12	52.29	3.93	9.12
H	CH <sub>2</sub> CF <sub>3</sub>	C <sub>12</sub> H <sub>9</sub> F <sub>3</sub> N <sub>2</sub> O <sub>2</sub>	296–8	91	50.36	3.17	9.79	50.78	3.39	9.91
Br	CH <sub>2</sub> CF <sub>3</sub>	C <sub>12</sub> H <sub>8</sub> BrF <sub>3</sub> N <sub>2</sub> O <sub>3</sub>	298–300	98	39.48	2.21	7.67	39.65	2.29	7.36
MeO	CH(CF <sub>3</sub> ) <sub>2</sub>	C <sub>14</sub> H <sub>10</sub> F <sub>6</sub> N <sub>2</sub> O <sub>4</sub>	296–8	70	43.76	2.62	7.29	43.94	2.81	6.89
Me	CH(CF <sub>3</sub> ) <sub>2</sub>	C <sub>14</sub> H <sub>10</sub> F <sub>6</sub> N <sub>2</sub> O <sub>3</sub>	>300	76	45.66	2.74	7.61	45.85	2.87	7.86
H	CH(CF <sub>3</sub> ) <sub>2</sub>	C <sub>13</sub> H <sub>8</sub> F <sub>6</sub> N <sub>2</sub> O <sub>3</sub>	294–6	75	44.08	2.28	7.91	44.55	2.37	7.73
Br	CH(CF <sub>3</sub> ) <sub>2</sub>	C <sub>13</sub> H <sub>7</sub> BrF <sub>6</sub> N <sub>2</sub> O <sub>3</sub>	300–2	73	36.05	1.63	6.47	36.18	1.80	6.35

<sup>a</sup> At >180°C, the compounds turned yellow, and all of them decompose at the mp.

0.2 mol) in dichloromethane (30 mL) in a 250 mL flask, a freshly prepared cyanoacetyl chloride (from cyanoacetic acid and phosphorus pentachloride) was added dropwise with stirring at ice bath temperature. After the addition was complete, the mixture was refluxed for 2 h and then stirred at rt for 16 h. Water (100 mL) was added with stirring, the mixture was filtered, the organic layer was collected, and the aqueous layer was extracted with CH<sub>2</sub>Cl<sub>2</sub> (2 × 20 mL). The combined organic solution was washed with 2 N H<sub>2</sub>SO<sub>4</sub> (10 × 50 mL) until it was free of dimethylaniline, then with water (2 × 50 mL), and with 10% sodium sulfate (50 mL). The inorganic salt was filtered, the solvent was evaporated, and the residue was distilled at reduced pressure, giving 10 g (30%) of the colorless ester, bp 76–78 °C at 1–2 Torr.

<sup>1</sup>H NMR (CDCl<sub>3</sub>, 298 K, 400 MHz) δ: 3.65 (2H, s), 4.59 (2H, q, *J* = 8.3 Hz). <sup>19</sup>F NMR (CDCl<sub>3</sub>, 298 K, 400 MHz) δ: -74.80 (t, *J* = 7.5 Hz). <sup>13</sup>C NMR (CDCl<sub>3</sub>, 298 K, 400 MHz) δ: 24.16 (t, *J* = 138 Hz), 61.64 (tq, *J*<sub>t</sub> = 152 Hz, *J*<sub>q</sub> = 37 Hz), 112.26 (t, *J* = 10.6 Hz), 122.26 (qt, *J*<sub>q</sub> = 277 Hz, *J*<sub>t</sub> = 4.7 Hz), 162.04 (m). Anal. Calcd for C<sub>8</sub>H<sub>8</sub>F<sub>3</sub>NO<sub>2</sub>: C, 35.94; H, 2.41; N, 8.38. Found: C, 35.68; H, 2.38; N, 8.13.

**Reaction of Trifluoroethyl Cyanoacetate and Aryl Isocyanates.** The following procedure is also representative for the reaction with *p*-Me, *p*-MeO, and *p*-Br phenyl isocyanates. A mixture of trifluoroethyl cyanoacetate (0.84 g, 5 mmol) and triethylamine (1.02 g, 10 mmol) in dry DMF (5 mL) was stirred for 5 min, PhNCO (0.59 g, 5 mmol) was added, and the solution was stirred for 6 h. Ice cooled 2 N HCl (50 mL) was then added with stirring. The white precipitate formed was filtered and dried in air to afford 1.3 g (91%) of the crude **6c**, mp 296–8 °C. Anal. Calcd for C<sub>12</sub>H<sub>9</sub>N<sub>2</sub>F<sub>3</sub>O<sub>3</sub>: C, 50.36; H, 3.17; N, 9.79. Found: C, 50.78; H, 3.39; N, 9.91. The NMR spectral data for **6a–d** are given in Tables 3–5 and S11–S13, and the mp and microanalysis are given in Table 11.

**1,1,1,3,3,3-Hexafluoroisopropyl Cyanoacetate.** 1,1,1,3,3,3-Hexafluoroisopropyl cyanoacetate was prepared according to the procedure described above for preparing trifluoroethyl cyanoacetate. Bp 60–2 °C/7 mmHg. Yield 16%. <sup>1</sup>H NMR (CDCl<sub>3</sub>, 298 K, 400 MHz) δ: 3.77 (2H, s), 5.80 (1H, heptet, *J* = 5.8 Hz). <sup>19</sup>F NMR (CDCl<sub>3</sub>, 298 K, 400 MHz) δ: -74.23 (d, *J*

= 5.6 Hz). <sup>13</sup>C NMR (CDCl<sub>3</sub>, 298 K, 400 MHz) δ: 24.00 (t, *J* = 138 Hz), 67.83 (dm, *J*<sub>d</sub> = 152 Hz, *J*<sub>m</sub> = 35 Hz), 111.46 (t, *J* = 10 Hz), 119.86 (qm, *J*<sub>q</sub> = 282 Hz), 161.07 (m). Anal. Calcd for C<sub>6</sub>H<sub>5</sub>F<sub>6</sub>NO<sub>2</sub>: C, 30.66; H, 1.29; N, 5.96. Found: C, 30.95; H, 1.23, N, 5.80.

**Reaction of Hexafluoroisopropyl Cyanoacetate with Phenyl Isocyanate.** (a) *Reaction with Phenyl Isocyanate.* To a stirred solution of hexafluoroisopropyl cyanoacetate (0.59 g, 2.5 mmol) and triethylamine (0.51 g, 5 mmol) in THF (5 mL), phenyl isocyanate (0.29 g, 2.5 mmol) was added, and the mixture was stirred for 24 h at rt and then poured into ice-cooled 2 N HCl (50 mL) with stirring. The white precipitate formed was filtered and washed with water to give 0.66 g (75%) of **9c**. Crystallization from ethyl acetate gave white needles, mp 294–6 °C. Anal. Calcd for C<sub>13</sub>H<sub>8</sub>F<sub>6</sub>NO<sub>3</sub>: C, 44.08; H, 2.28; N, 7.91. Found: C, 44.55; H, 2.37; N, 7.73.

(b) *Reaction with Other Aryl Isocyanates.* The same procedure was applied for *p*-methoxyphenyl isocyanate (0.37 g), giving **9a** (0.67 g), for *p*-methyl isocyanate (0.33 g), giving **9b** (0.79 g), and for *p*-bromophenyl isocyanate (0.5 g), giving **9d** (0.8 g). Mps and microanalysis of all compounds are in Table 11, and <sup>1</sup>H, <sup>13</sup>C, and <sup>19</sup>F NMR spectra are in Tables 3–5 and S11–S13.

**Acknowledgment.** We are indebted to Professor Silvio Biali for discussions, to Dr. Shmuel Cohen for the X-ray structure determination, and to the Israel Science Foundation for support. D.C. thanks the financial support of the MUIR COFIN 2001, Rome.

**Supporting Information Available:** Figures S1–S3 of ORTEP of **Z-7a** and stereoviews of **Z-7a** and **Z-9b**, Tables S1–S10 of crystallographic data for **Z-7a** and **Z-9b**, and Tables S11–S13 of <sup>1</sup>H, <sup>13</sup>C, and <sup>19</sup>F NMR data. This material is available free of charge via the Internet at <http://pubs.acs.org>.

JO020464A